PROBING THE DISTRIBUTION OF GLIADIN PROTEINS IN DOUGH AND BAKED BREAD SAMPLES USING CONJUGATED QUANTUM DOTS AS A LABELING TOOL

BY
SHADI ANSARI

THESIS
Submitted in partial fulfillment of the requirements
for the degree of Master of Science in Food Science and Human Nutrition
with a concentration in Food Science
in the Graduate College of the
University of Illinois at Urbana-Champaign, 2013

Urbana, Illinois

Master's Committee:
Professor Jozef Kokini, Chair
Professor Nicki Engeseth
Associate Professor Hao Feng

Abstract

Quantum dots (QDs) technology is commonly used in medical application as a probe for diagnostic procedures via imaging macroscopic and microscopic structures in life sciences. Also they can be used for designing of biosensors. However, the application of this technology is very new in food science . In this study, a novel application of QDs in food science was investigated. QDs were conjugated to gliadin antibody and used as a fluorescent probe to track gliadin protein in dough and baked bread samples. The type and quantity of gluten proteins and their subfractions, gliadins and glutenins, are critical for baked product functionality. Gliadin proteins are also able to activate coeliac disease which causes severe damages to the digestive system. Therefore, it is important to understand how gliadins are distributed in dough and the effect of baking conditions on distribution of gliadin in baked bread. QDs conjugated gliadin antibody was specifically bound to gliadin to determine its distribution in three different samples prepared at various heating times. Dough, bread baked at 5 minutes and at 9 minutes were evaluated. Three different layers (i.e. top, center and bottom) were investigated. Top layer in baked breads means the layer which is far from the direct heat then center layer and closet layer to heat is bottom layer of baked breads. The conjugation process was through covalent linkage in presence of SMCC (Succinimidyl-4-(N-maleimidomethyl) cyclohexane-1-carboxylat) cross linker.

Confocal laser scanning microscopy (CLSM) was used to image QDs conjugated with gliadin antibodies. The mean intensity of gliadin attached to quantum dots for each sample was calculated and plotted. CLSM images showed significant changes in the distribution of gliadin with baking time compared wheat flour dough. Bread baked at 9 minutes shows the highest amount of fluorescent intensity from gliadin bound quantum dots in the top layer which

is not in contact with the direct heat. Similar observation was made for bread baked at 5 minutes and both contained more gliadin than dough sample. However, the amount of gliadin in dough is more than that of bottom layers which receive more heat in both baked bread samples. Analysis of variance (ANOVA) was conducted to compare the mean fluorescence intensity of QDs bound to gliadin in different samples and sections. The ANOVA analysis of the overall data with probability of 99% (α=0.01) and 95% (α=0.05) indicated that the mean intensity value of gliadin changes was statistically significant.

To my parents, brother, sister and Abdolreza

for theirs endless love and support

Acknowledgment

I would especially like to thank Dr. Jozef Kokini my adviser, for his guidance and assistance during the research and preparation of my thesis.

I would also like to thank Dr. Nicki Engeseth and Dr. Hao Feng for serving on my graduate committee and providing helpful suggestions and comments on this project.

I also wish to thank Dr. Peter Yau at biotechnology center and Dr. Mayandi Sivaguru at Institute of Genomic Biology (IGB) for their mentoring and guidance during my research at UIUC.

Special thanks to all my colleagues whose thoughtful discussions contributed greatly to my education, especially Dr. Nesli Sozer, Fatih Bozkurt, Gizem Gezer, Suzan Uzun.

I owe the most thankful to my parents, Ali and Zari, for their unconditional love and support. It is really hard for me to put my gratitude to them into words. Many thanks to my brother and sister, Hadi and Nazli for their continues supports.

I would especially like to thank my husband, Abdolreza, for his love, support and understanding in this very demanding period of life. He has always inspired me throughout this process.

Table of Contents

Chapter One:

Introduction

The wheat storage proteins are called glutens, and can be classified into two groups, gliadins and glutenins. Glutenin subunits give elasticity to gluten proteins and are subdivided into low-molecular weight (LMW) and high-molecular weight (HMW) glutenins. They build polymeric proteins through intermolecular disulfide bounds (Loussert et al., 2008). However, gliadins are monomeric and generally contribute to viscosity of gluten proteins. Gliadins are soluble in aqueous alcohols. Reversed-phase HPLC can separate gliadins into more than 30 components based on their polarity (Varriale et al., 2007). According to their relative mobilities, gliadins are subdivided into four groups, α-, β-, γ- and ω-gliadins (Li et al., 2008).

Composition and quantity of gliadin and glutenin proteins are very important to wheat quality. Gliadins account for about 50 % of wheat grain and glutenins account for 35 % of total proteins (Leszczynska et al., 2008).

The quality of a baked bread product depends on the properties of the dough during processing. Dough is a complex system and generally consists of a hydrated gluten matrix with embedded starch particles (Transmo et al., 2003). The hydrated protein aggregates, and the starch matrix and starch-protein interactions give rise to very unique viscoelastic properties and all these macromolecular interactions affect the rheology, fundamentally. The interactions between starch-starch are Van der Waals and hydrogen bonding interactions. However, the gluten proteins have unique properties. In these proteins, disulfide bonds between subunits, hydrogen bonds, entanglements ionic and hydrophobic interactions form a large continuous network (Transmo et al., 2003).

Previous experiment and studies have shown that the baking quality of different flours depend on protein content, size distribution and properties of gluten macromolecules (MacRitchie, 1992 and Magnus et al., 2000).

Gliadin proteins are primarily responsible for celiac disease (CD) (Varrial et al., 2007). Celiac disease is an inflammatory disease of the small intestine which prevents it from absorbing parts of food that are important for proper nutrition. The inflammation and its impact on digestion are due to an inflammatory reaction caused by gluten consumption. Therefore, developing immunoassays which are able to exactly determine the content of gluten proteins are very important and remains a hard task.

Gliadin is a complex mixture of proteins and difficult to solubilize and extract from wheat flour. Therefore, it is challenging to develop any assay which is able to accurately quantify gliadin content in food for celiac patients (Varriale et al., 2007). Until now, none of the available methods are considered to be fully satisfactory. There are a series of enzyme-linked immunoadsorbent assays (ELISAs) that have been developed for the analysis of gliadin in food (Rumbo et al., 2001). However, there are some concerns about the usefulness of these immunoassays. The use of reducing agent in these methods improves the extraction of prolamins but impacts the immunochemical quantification.

In this study, we considered a novel approach by utilizing immunoglobulins that are tagged with fluorescent semiconductor nanocrystal known as quantum dots (QDs) as a labeling tool for gliadin proteins. QDs were conjugated to gliadin antibody and visualized by confocal laser scanning microscopy (CLSM) to identify the distribution of gliadin proteins in dough and flat bread samples.

Chapter Two:

Literature Review

2.1. Wheat Gluten Protein

Based on intensive studies in the last 90 years, wheat proteins are the best known among cereal proteins. Wheat proteins have shown a lot of chemical diversity and complexity with a growing number of in depth investigations with the merging variety new scientific tools for separation and isolation. Improved methods for separation of wheat proteins were developed and provided increasingly more accurate explanation of the structure of gluten protein (Lasztity, 1996).

It is well accepted that wheat storage proteins gluten and their subfractions, gliadins and glutenins are closely related to flour quality and baking performance (Hoseney et al 1970; Kokini et al., 1994P; Micard and Guilbert, 2000; Orth and Bushuk, 1972; Schofield et al 1983; Shewry and Tatham, 1990Wrigley 1970; Wrigley et al., 1982; Wrigley et al., 2006). Results from early investigations suggested that the ratio of gliadin to glutenin was the main factor in gluten properties affecting baked product quality. The strength of the gluten complex is dependent on the rheological properties and extensibility in particular of glutenin and gliadin (Wrigley et al, 2006). Figure 1 shows the model of interactions of wheat protein in dough (Wall, 1979).

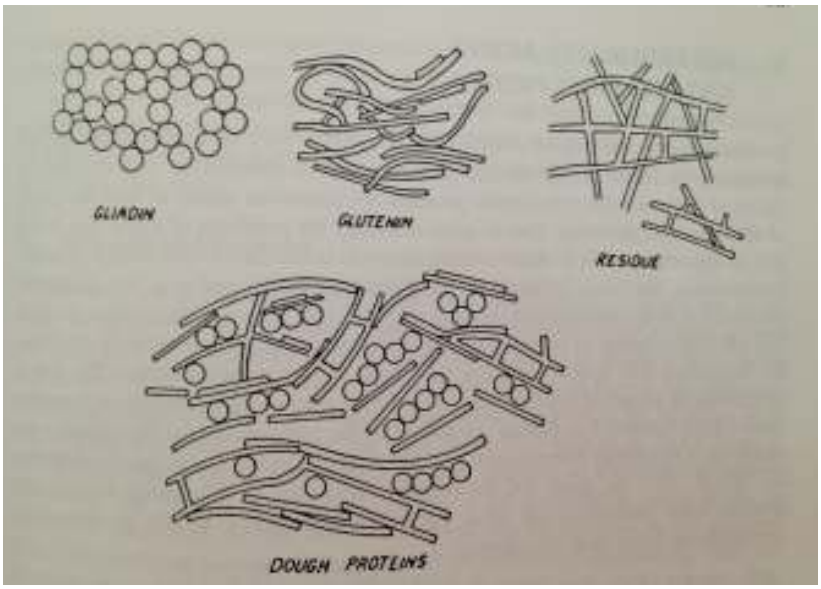

Figure 1. Model of interactions of wheat proteins in dough (Wall, 1979).

2.2. Gliadin Protein

Gliadin is the most abundant storage protein of the wheat seed, amounting to about 40% by weight of wheat flour protein. It was the first subfraction of gluten protein to be studied and named in the early 19th century, because its extraction and purification was relatively easier than the wide range of glutenin subfractions (Orth and Bushuk, 1972; Wieser, 2007).

Gliadin is one of the major protein components of the human diet of many societies. The molecular mass of gliadin polypeptides ranges from 15 to 60 kDa but most are in the narrow range of 25-40 kDa. Gliadin polypeotides have a low content of charged aminoacids and they form only intramolecular disulfide bonds. Therefore, they are assumed to exist as largely as monomeric molecules in their native states (Wrigley et al, 2006). Madeka and kokini 1994 studied the various phase changes in gliadin and demonstrated that at increasing temperatures it is possible to complex gliadin molecules to form a high molecular network.

Different techniques have been used to study gliadin polypeptides, including modifications of one-dimensional electrophoresis (Woychik et al 1961; Autran and Bourdet 1975; Kasarda et al 1976; Shewry et al 1978; Autran et al 1979; duCros and Wrigley 1979; Lookhart et al 1982) two-dimensional electrophoresis (Wrigley 1970; Mecham et al 1978; Payne et al 1982; Novoselskaya et al 1983; Payne et al 1985) and high performance liquid chromatography (Bietz and Burnout 1985; Scanlon and Bushuk 1990; Larre et al 1991). However, polyacrylamide gel electrophoresis (PAGE) as a preferred method was used to evaluate gliadin from large numbers of samples or from complex experiments (Wrigley et al, 2006). PAGE is widely used in the US and in many countries in Europe for separation of gliadins.

Based on electrophoretic mobility at acidic pH (pH: 3.2) the wheat gliadins may be separated into the slowest group named ω-gliadin and three faster groups named α-, β- and γ-gliadins. Comparisons of amino acid and DNA sequences show that the α- and β- gliadins are closely related and referred to as ‘‘α- type’’ gliadins, while the γ- and ω-gliadins are structurally distinct. The α -type gliadins consist of a short N-terminal domain of five residues, a repetitive domain of about 113–134 residues and a C-terminal domain of about 144–166 residues, the latter domain containing two poly-glutamine regions. The repetitive domain consists of a repeat motif of five to eight residues of consensus sequence Pro(Phe/Tyr)ProGlnGlnGln(Gln)(Gln), and differences in the length of the repetitive domain define the differences in molecular weight of the α -gliadins. The γ -type gliadins have a similar domain structure consisting of a 12-residue N-terminal domain, a repetitive domain of 78–161 residues with a consensus repeat consisting of ProPheProGlnGln(Gln)ProGlnGln(ProGlnGln), and a C-terminal domain of 135–149 residues containing a single poly-glutamine region. Differences in the length of the repetitive domain

account for the variation in the molecular weight range (about 26,000–36,000) of the γ -type gliadins. There are few complete sequences available for the ω -gliadins. One consists of a short N-terminal domain of 11 residues, a repetitive domain of 238 residues, and a short C-terminal domain of 12 residues; the consensus repeat consists of 6–11 residues of ProPhe ProGln(Gln)(Gln)ProGln(Gln)(Gln)(Gln) and is similar to the γ -gliadin repeat (Shewry et al. 2008; Tatham and Shewry 1995; Hsia and Anderson 2001; Matsuo et al. 2005; Altenbach and Kothari 2007). The structures and/or sequences of the gliadin repetitive domains are causative factors in a number of human diseases. The immunodominant activating sequences in coeliac disease are located in repetitive domains of the ω -gliadins (Ang et al., 2010).

Gliadins may be divided into sulfur rich (α-, β- and γ-gliadins) and S-poor (ω-gliadin) due to difference in cystein content in gliadin components. All gliadin components have extremely high glutamic acid content. In some ω-gliadin, the glutamic acid content is higher than 50%. Almost all of the glutamic acid content in gliadin is present as glutamine. The amino acid compositions of isolated α-, β-, γ-and ω-gliadin were determined and published (Lasztity, 1996). The high content of proline in all gliadins has an effect on the secondary structure of gliadin polypeptide since the formation of α-helices is disrupted by the presence of proline side chains. Gliadins are poor in basic amino acids, especially lysine. Gliadins are among the least charged proteins known, due to the low level of lysine, arginine, and histidine along with low levels of free carboxyl groups.

On the basis of molecular weight, the gliadin components may be divided into two groups. α-, β- and γ-gliadins have molecular weight of about 30 kDa. The molecular weight of ω-gliadin is approximately 60 kDa, twice as high as those of α-, β- and γ-gliadins. The investigation of the primary structure (i.e the sequence of gliadins components) began in 1974

with the work of Kasarda et al. The N-terminal sequence of α-gliadin components and other gliadins were investigated (Lasztity, 1996).

A number of studies have reported the conformation of gliadins. Krejci and Svedberg (1935) used analytical ultracentrifugation to analyze the gliadin fraction of wheat extracted with aqueous ethanol. This study demonstrated the heterogeneous nature of wheat gliadins and calculated the dissymmetry factor which indicated the non-globular nature of these proteins. Also, Lamm and Poulsen (1936) and Entrikin (1941) analyzed the shapes of gliadins using translational diffusion and dielectric dispersion and showed asymmetric molecules. However, later measurements based on intrinsic viscosity indicated more globular structures (Taylor and Cluskey 1962; Wu and Dimler 1964; Cole et al. 1984). Field et al. (1986) determined the intrinsic viscosity of the ω-gliadin homologue from barley and described a rod-shaped molecule. However, Thomson et al. (1999) used small-angle X-ray scattering to study the size and shape of α-, γ- and ω-gliadins and described prolate ellipsoids of differing axial ratio. Both intrinsic viscosity and X-ray scattering require relatively high concentrations of protein in contrast to analytical ultracentrifugation. At higher concentrations, aggregation can become problematic and may account for the apparent disparity in the results. However, advantage can be taken of recent developments in analytical ultracentrifugation procedures to study of the size and shape of different gliadins fractions in dilute solution conditions. Although the principles of both sedimentation velocity and sedimentation equilibrium methodology in the ultracentrifuge are essentially the same as at the time of Krejci and Svedberg (1935), the instrumentation, data capture and analysis software have advanced enormously (Scott and Schuck, 2005).

2.3. Disulfide Bonds

The most important covalent bonds in cereal proteins are disulfide linkages. The disulfide bonds present in cystein residues are a common feature of the majority of proteins and serve to stabilize a variety of molecular structure. A cystine residues crosslink polypeptide chain in gliadin and glutenin proteins is shown in Figure 2 (Wall, 1971). Disulfide linkage in gliadin proteins is primarily intramolecular, whereas in glutenin they are both intermolecular and intramolecular, as (Kokini et al., 1994).

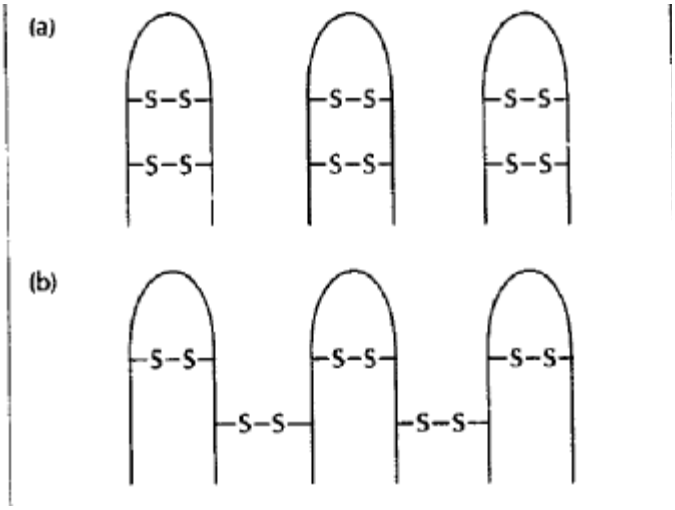

Figure 2. Disuilfied bonds in cereal proteins: a) Intramolecular bonds in wheat gliadin b) intramolecular and crosslinks in wheat glutenin (Wall, 1971 and Kokini et al., 1994).

There is no doubt that thiol groups and disulfide bonds play an important role in determining gluten and dough properties. There are some useful data based on studying changes in rheological properties due to the deformation of disulfide bonds (Lasztity, 1996). The disulfide bond in gluten and dough form a dynamically changing system. The changes are related to both the quantity and the distribution of the S-S linkages. Gliadin showed a maximum

crosslinking density at 100°C calculated using G' and density data (Madeka and Kokini, 1994). The thiol groups may affect the disulfide bonds in oxidation of new disulfide bonds which may be formed and interchange reaction may occur between S-S bonds and thiol groups which causes a dynamic change in the distribution of disulfide linkages. Conversely, a reduction of disulfide bonds causes an increase of SH groups. Oxidation strongly affects rheological properties of dough. When thiol groups and converted into disulfide bonds especially intramolecular disulfide bonds a high molecular weight crosslinked network is formed (Madeka and Kokini, 1994) and rheological properties increase by several orders of magnitude. Conversely when disulfide bonds are converted into thiol groups there is a dramatic drop in rheological properties. Although the importance of disulfide bonds in the determination of rheological properties of gluten proteins has been confirmed by many experimental facts, the investigation of the last few decades have shown that the explanation of rheological properties of gluten is not possible without taking into account the other possible interactions in the gluten network (Lasztity, 1996).

Research performed in the last few decades showed that gluten proteins contain a great number of side chain groups forming hydrogen bonds. For example, acidic, basic, amide and thiol and disulfide groups as functional groups were observed in gluten proteins (Pomeranz, 1968). The contribution of hydrogen bonds and reactive sulfur-containing groups of proteins to the rheological properties of dough were studied by Jankiewicz and Pomeranz in 1965. Vekar et al (1965) have reported that freshly washed gluten becomes stronger and more elastic after it is dipped into D_2O. These facts also indicate that hydrogen bonds play an important role in gluten structure.

In addition, gluten protein contains several amino acids with hydrophobic side chain such as alanin, leucine, phenylalanine, isoleucine, valine and proline which are participating in

forming hydrophobic bonds (Lasztity, 1996). Figure 3 shows the proposed structure of gluten complex (Lasztity, 1972).

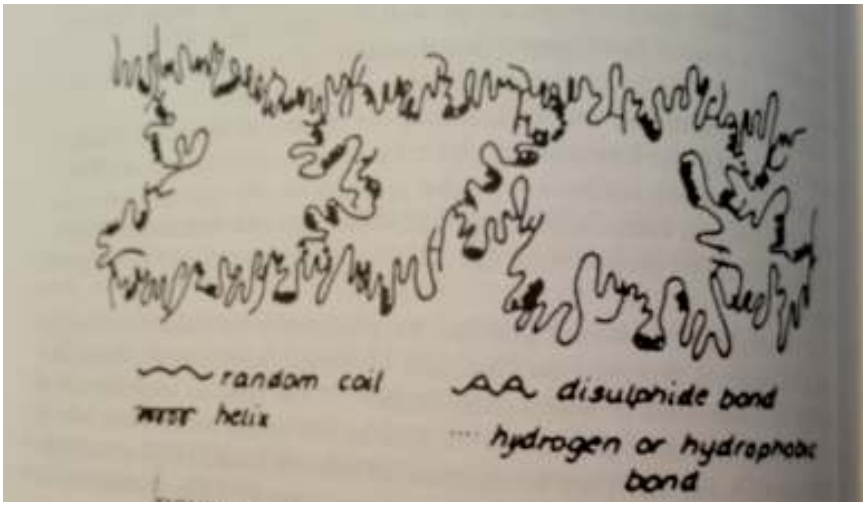

Figure 3. Proposed structure of gluten complex (Lasztity, 1972).

2.4. Dye Binding

Some techniques based on dye-binding capacity were used for measuring proteins in solution. Interaction with the proteins modifies the absorption spectrum of the dyes, and this allows quantification of the complex.

Coomassie Brilliant Blue stain is the absorption reactant most frequently used. Eynard et al (1994) studied the behavior of color development by dye-binding in gluten, gliadin, water and acid-soluble wheat proteins. Figure 4 shows the spectra of the dye without protein added and with bovine serum albumin (BSA), commercial gliadin, standard gluten, water and acid extracts of flour. It was shown that with all proteins, the absorbance of the neutral dye (λ_{max} 650 nm) significantly overlaps with that of the protein bound anion (λ_{max} 595 nm), whereas the 460 nm absorbance is due only to the cation. However, two major limitations were reported. 1) the amount of protein estimated depends on the type of protein used 2) color development is not

linear over wide ranges of protein concentrations. Also, color variability among different proteins is one of the most significant disadvantages of protein assays by dye binding using Coomassie Blue.

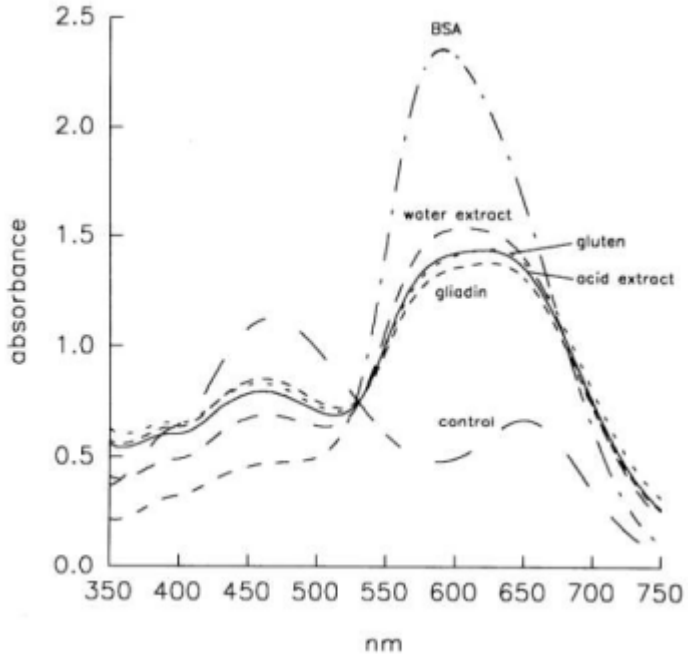

Figure 4. Spectra of Bradford reagent with and without protein added (Eynard et al., 1994).

2.5. Microscopy Techniques

Transmission Electron Microscopy (TEM) has been used in the past to examine the structure of gluten. However, it was unable to directly visualize specific groups of proteins. It has not been possible to elucidate the structure of the glutenin polymers using traditional techniques such as X-RAY crystallography because the gluten network can not be crystallized. Other techniques such as circular dichroism spectroscopy, Figure 5 (Tathman and Shewry, 1985), infrared spectroscopy, Figure 6 (Pezolet et al., 1992) and scanning tunneling microscopy, Figure 7 (Miles et al., 1991) have been used to study the structure of isolated gluten polypeptides.

However, these techniques are not applicable to understanding the structure of gluten in dough (Lindsay and Skerritt, 2000).

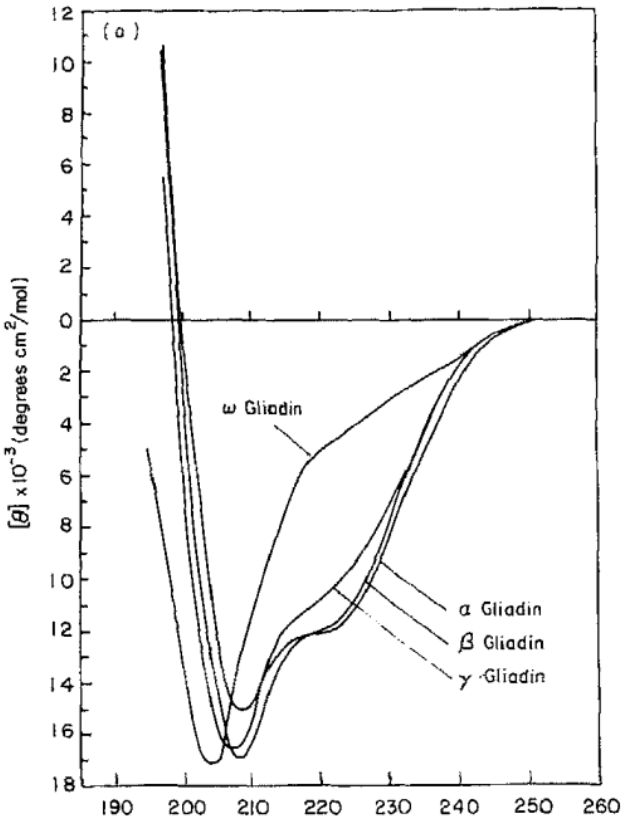

Figure 5. The circular dichroism spectra of α-, β-, γ- and ω -gliadins in 70% (v/ v) aqueous ethanol (Tatham and Shewry, 1985).

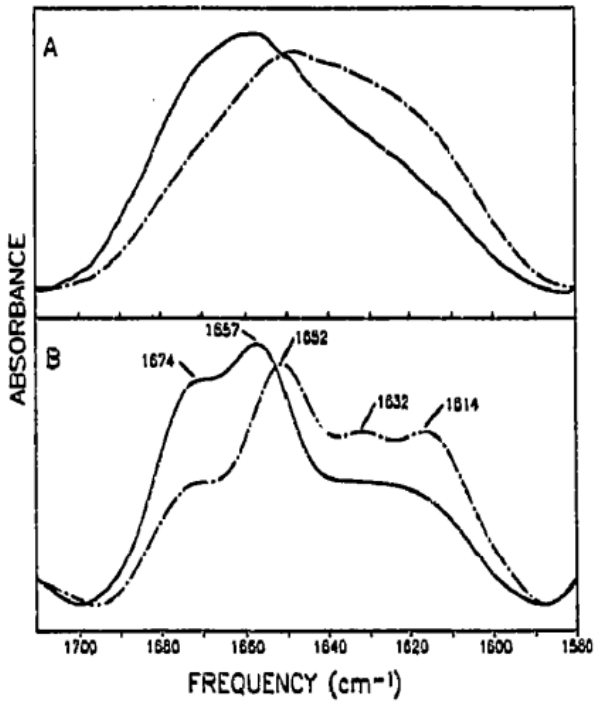

Figure 6. I (A) Original and (B) Fourier deconvolved infrared spectra in the amide I region of wheat gluten in the doughy state (-,-,-) and in solution in 0.1 M acetic acid (----) (Pezolet et al., 1992).

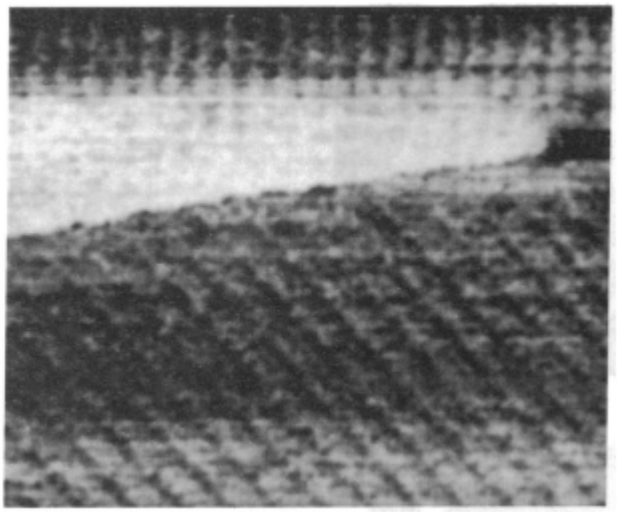

Figure 7. Unprocessed STM image (60 nm x 41 nm) of HMW subunit protein molecules, showing two ordered domains of rod-like molecules (Miles et al., 1991).

Confocal Laser Scanning microscopy (CLSM) is a relatively new and effective optical tool which has been used with food materials since the 1990s. In contrast to conventional light microscopy, the light source is replaced by a laser, a scanning unit and pinhole to improve the limited depth of focus. Not only thin sample but also thick food sample can be analyzed by CLSM to obtain structural information. The primary value of using CLSM in dough and baked product research is its ability to produce three-dimensional information on the properties of protein and starch networks in wheat products. CLSM enables excellent resolution within the plane of sections and also between section planes (Durrenberger et al., 2001). Figure 8 shows the confocal microscopy image of wheat dough (Bugusu et al., 2002).

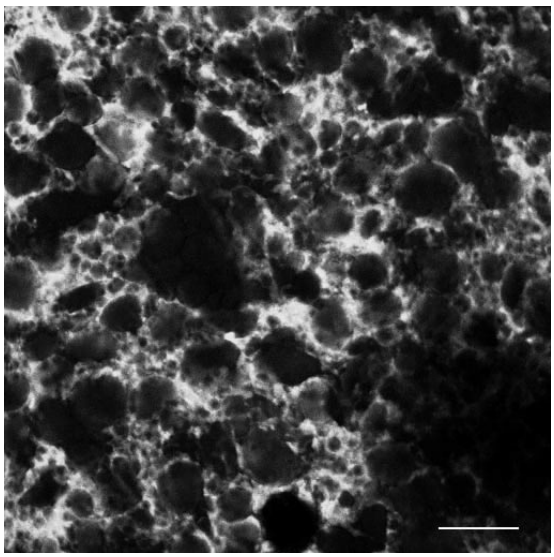

Figure 8. Confocal scanning laser micrograph of wheat dough- gluten networks (white) stained with fluorescein isothiocyanate. Size of the bar = 50 μm (Bugusu et al., 2002).

2.6. Effect of Heat on Gluten Protein

The effect of heat on gluten have been shown to be of critical importance for baking functionality, producing heat denaturation of protein and accompanying rheological and functional changes. Booth et al. (1980) and Schofield and Booth (1983) showed the decrease in baking functionality of gluten during heating with decrease in solubility and extractability. However, cross linking and polymerization of gluten polymer attributed to increase in sulfhydryl (SH) - disulfide (SS) interchange reactions increased.

Kokini et al. (1994) showed the temperature-induced reaction zones in gliadin. They demonstrated in the temperature range 50-70°C, G' (elastic modulus) was roughly equal to G" (viscose modulus). However, a large increase in G' was observed at temperatures above 70°C. The increase in elastic modulus can be attributed to cross link reactions occurring among gliadin molecules resulting in the formation of network structure. On further heating until 120°C, G' was at its maximum value whereas G" fell to a minimum value. At this point, it seems the aggregation reaction has been completed and a highly cross linked network formed. They showed a reduction in G' and simultaneously peak in G" in the temperature even further, so that the softening of gliadin was observed at 130°C. Also, Hayta and Schofield (2005) showed that the greatest change in the rheological behavior of gluten is in the temperature range of 30°C - 90°C. It seems the changes in the elastic modules as the change in G' are greater than the changes in G".

Guerrieri et al. (1996) observed heat induced changes in surface hydrophobicity of gluten. Stathopoulos et al. (2008) showed that the temperature at which heat-induced changes occur depend on the variety of wheat protein. Ponomarev and Lifanova (1951 and 1956) investigated the physicochemical properties of gliadin upon heat denaturation. During heat

denaturation of protein a change occurs in a whole series of its physicochemical properties such as solubility, optical activity, water absorption capacity and swelling. Any of these properties can be chosen as an index of the rate of heat denaturation. Ponomarev and Lifanova (1951 and 1956) determined changes in gliadin optical activity during heat denaturation. For simplicity of calculation all angles of rotation were given in the first quadrant, that is $[\alpha]=180-[\alpha]'$. Since they defined the kinetic of heat denaturation of gliadin by an equation analogous to the equation for a monomolecular reaction, a proportionality exists between the value $[\alpha]'$ and the amount of gliadin being denaturated, which is $d\alpha/dt= K (\alpha_0-\alpha_t)$. They determined the percentage of changing in angle of rotation of a gliadin solution during denaturation from the initial and found that the denaturation of protein during heating depends on both temperature and time of heating. The values obtained in Table 1 by Ponomarev and Lifanova (1956) showed that the rate constant of heat denaturation of gliadin proteins changed very little with time of denaturation but increased with temperature of denaturation.

Equation 1. $K=1/t \ln \alpha_0/\alpha_t$

In this equation K is rate constant of gliadin denaturation, t is time of denaturation and α_0/α_t shows the optical activity changes during denaturation.

Table 1. Rate constant of gliadin denaturation (Ponomarev and Lifanova, 1956)

Values	**Denaturation Temperature, 70°C**		**Denaturation Temperature, 130°C**	
	60 min	120 min	60 min	120 min
K	0.00512	0.00560	0.01435	0.01054

The changes induced by heat eventually lead to networks of large gluten protein by formation of gliadin-glutenin bonds through SS cross linking in the process. The polymerization of glutenin may involve oxidation and sulfhydryl-disulfide SH-SS exchange reactions. Heating at 95°C resulted in polymerization of both gliadin and glutenin which caused increase in viscosity using Rapid Visco Analyzer (RPV) profile (Sathopulos et al., 2006). Madeka and Kokini (1994) demonstrated a networking reaction for gliadin with 15-40% moisture in the temperature range of 70-115°C. Weegels et al. (1994) showed that in heated gluten, free SH groups decreased and disulfide bonds increased. Schofield et al. (1983) proposed a sulhydryl-disulfide SH-S-S exchange reaction mechanism. They concluded that the total level of free SH groups remained constant irrespective of the temperature. Moreover, Lagrain et al. (2008) investigated the importance of free SH groups at room temperature, at 90°C and after 15 minutes at 95°C. They concluded that at any time during hydrothermal temperature, free SH groups initiate gliadin-glutenin reactions at temperatures exceeding 90°C. The extent of these reactions depends on the available concentration of free SH groups in the system. The model for gliadin-glutenin cross linking process proposed by Lagrain et al. (2008) is shown in Figure 9. As it has shown in Figure 9 (I.1) in the absence of additives, heating to 90C first resulted in conformational changes, exposing previously unavailable areas possibly containing free SH-groups and, next, polymerization of glutenin with oxidation of most but not all SH-groups. At 90C, still some free SH-groups can be measured. However, in Figure 9 (I.2) at temperatures exceeding 90C, these free SH-groups of glutenin can induce a covalent linkage with gliadin through a heat-induced SH-SS exchange mechanism. This exchange reaction is catalyzed by SH-groups and readily occurs in (other) proteins at higher temperatures. The free SH-group carries out nucleophilic attack on the sulfur atom of a disulfide. It is probable that conformational changes

at 90C in the gluten proteins are necessary for gliadin–glutenin cross linking. Although there are many studies on the effect of heat on gluten protein, no established general rule were found.

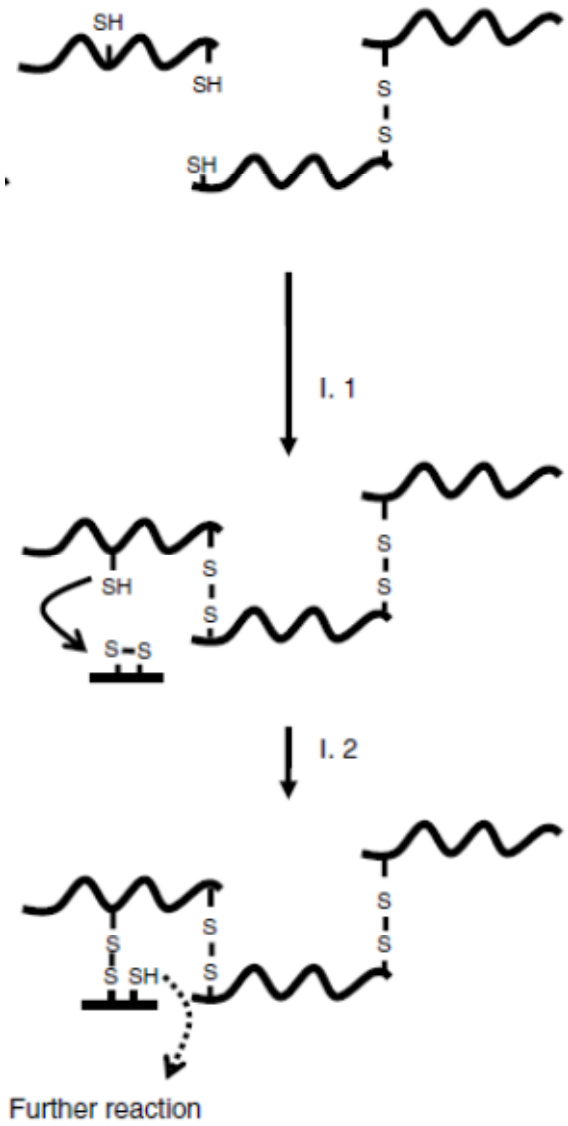

Figure 9. Model for gliadin-glutenin cross linking through SH-SS exchange reaction during hydrothermal treatment. (I.1) In the absence of additives, heating to 90°C leads to conformational changes exposing previously unavailable free SH-groups and polymerization of glutenin with oxidation of SH groups. (I.2) Glutenin can link to gliadin at temperatures exceeding 90°C through a SH-SS exchange reaction and the generated free SH group can react further with either gliadin or glutenin (Lagrain et al., 2008).

2.7. Immunochemical Methods

Among different analytical techniques, immunochemical methods are the most used to detect allergenic proteins and improve gluten-free products. The development of highly sensitive immunoassay for gliadin is of crucial importance for the management of a gluten-free diet since, a very small amount of gliadin can cause a severe immune response. Immunochemical methods recognize toxic proteins by mono or polyclonal antibodies (Rumbo et al., 2001).

Song et al. (1998) demonstrated the correlation between antibody binding and wheat quality which varies with the type of antibody and quality parameter. Their result showed that correlation between the antigen-antibody reaction and the wheat quality varied with the type of antibodies used and quality. The correlation coefficient obtained by polyclonal antibody (0.894) is slightly higher than monoclonal antibody (0.774). Also, the correlation coefficient between the antibody binding and protein content (0.762), wet/dry gluten content was high (0.894 and 0.887, respectively) while that between antibody binding and bread characters (bread volume (0.459) and bread ratio volume (0.474)) was low. Li et al. (2008) also showed relationship between polyclonal antibody and some major wheat quality parameters, such as development time, stability, strength and water absorption providing a basic tool for predicting wheat quality parameters instead of measuring them with instruments.

In many studies enzyme-linked immunosorbent assay (ELISA) was used to analyze the effect of heat on gliadin molecular changes. ELISA is a test that uses antibodies and color change to identify the presence of a substance. Rumbo et al. (2001) used four different anti-gliadin monoclonal antibodies and anti-gliadin serum and two different samples, purified gliadin and model dough simulating a baking process to analyze the effect of heat treatment. The result with purified gliadin showed that there is no particularly heat stable fraction. Heated dough

sample showed the impairment of protein extraction depending on the intensity of treatment. The impairment of the gliadin extraction caused by heat treatment during food manufacturing is the main problem in immunochemical quantification. Also, it is not possible to estimate its magnitude. Because it depends on the time-temperature condition used, the food matrix and the antibody that is used in immunochemical assays. Figure 10 shows the Immunochemical reactivity of heat-treated purified gliadin fractions measured using four different mAbs (monoclonal antibodies) and the anti-gliadin serum (Rumbo et al., 2001).

Lindsay and Skerritt (2000) used gold labeled secondary antibody to examine the changes in the structure of dough during mixing. The distribution of gold labeled antibody is indicative of the distribution of glutenin subunits in the sections. Figure 11 shows the pattern of gold label distribution characteristic of gliadins on sections of fixed dough. Differences in distribution of gold labeled antibody were observed on sections where for gliadin was present, low molecular weight glutenin subunits (LMW-GS) and high molecular weight subunits (HMW-GS) indicated that there are differences in the distribution of the different glutenin subunits and gliadin in wheat flour dough. Their result advanced understanding of the possible mechanisms of HMW-GS, LMW-GS and gliadins affect dough properties.

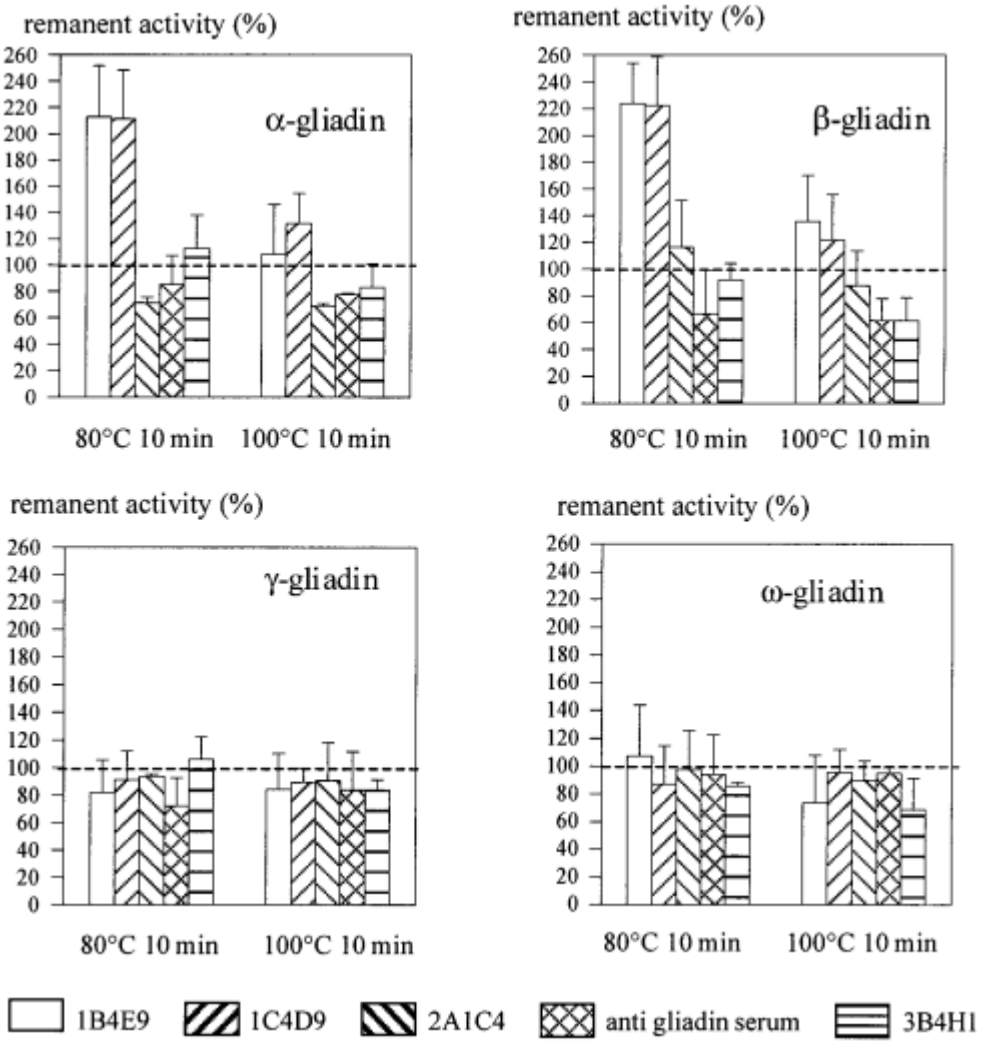

Figure 10. Immunochemical reactivity of heat-treated purified gliadin fractions measured using four different mAbs and the anti-gliadin serum. The time - temperature conditions, fraction analyzed, and antibodies used are indicated. Results are expressed as percentage (remanent reactivity) referred to the unheated control (100% of reactivity) (Rumbo et al., 2001).

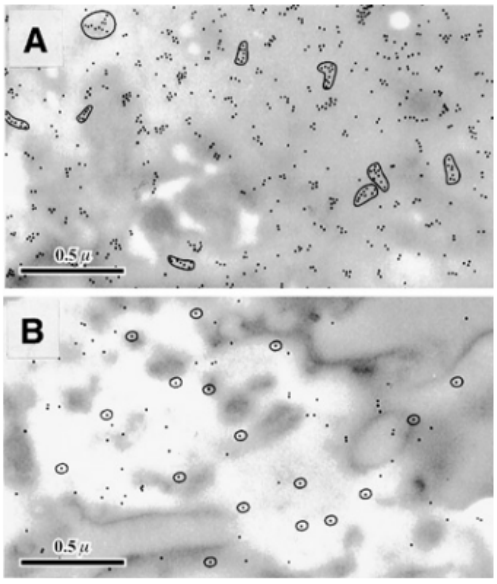

Figure 11. Pattern of gold label distribution (indicated with circles) characteristic of gliadins on sections of fixed dough. A, Chain or cluster association labeled with polyclonal antibody PAb to γ-gliadin N-terminal peptide., B, individual particles labeled with monoclonal antibody MAb40308 (Lindsay and Skerritt, 2000).

Gan et al. (1990) and Parker et al. (1990) used an indirect two step immunolabeling procedure with colloidal gold as an identifiable marker for electron microscopy to locate gluten protein in wheat flour dough and bread. Parker et al. (1990) produced an anti-gliadin monoclonal antibody (IFRN 0033). Cells producing antibody were selected using a microtitration plate enzyme-linked immunosorbent assay (ELISA) employing adsorbed gliadins as the solid phase. IFRN 0033 was found to be of the IgM subclass. Wheat endosperm were incubated in the monoclonal antibody IFRN 0033, followed by incubation in a 15 nm gold probe-labeled second antibody, only the storage protein bodies showed specific immunolabeling with gold particles (Figure 12). In their results, gliadin was only found on the cut surface of bread crumb not on the gas cell interface. They concluded that during dough formation, the stretched gluten proteins become aligned burying the epitopes in the gluten and making them inaccessible to antibody.

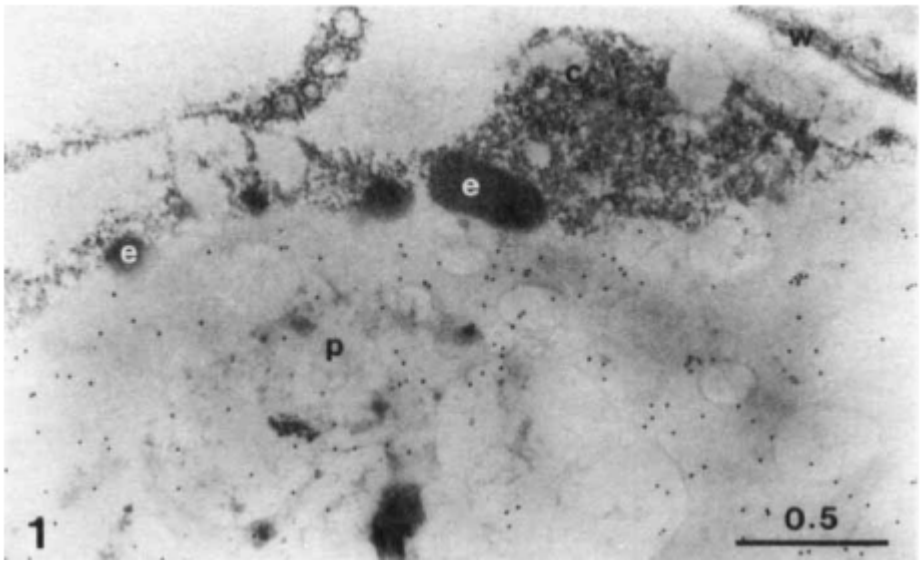

Figure 12. Section of endosperm of Avalon harvested 33 days after anthesis, showing immunogold labeling of protein within the protein body (p). The cytoplasm, cell wall and electron-opaque bodies are not immunolabeled. C, Cytoplasm; e, electron-opaque body; p, protein body; w, wall. Bar marker 0.5 μm (Parker et al., 1990).

2.8. Fluorescence Labeling Technique

Li et al. (2004) studied the dynamic surface and rheological properties of purified gliadin and glutenin with a fluorescence labeling technique and investigated with CLSM to locate gluten protein components and polar and nonpolar lipids in dough. They used tetramethylrhodamine B as a labeling tool. They found that gliadin was found not only in strands of dough but also in gas cell walls. However, glutenin was only found in bulk dough. Figure 13 shows the CLSM of the control bread dough. Also, Figure 14 shows the fluorescence intensity of gliadin in dough at different depths from surface of the dough to a depth of 1.2 mm (Li et al., 2004).

Varriale et al. (2007) investigated an essay which is based on the measurement of the fluctuations of fluorescein-labeled gliadin peptides with fluorescence correlation spectroscopy

(FCS) in the absence and presence of anti-gliadin antibodies. They labeled gliadin peptides with fluorescein-5-isothiocyanate (FITC). They obtained a detection limit of 0.006 ppm in gluten with combination IgG antibody with the fluorescence immunoassay which is lower than previous studies with ELISA.

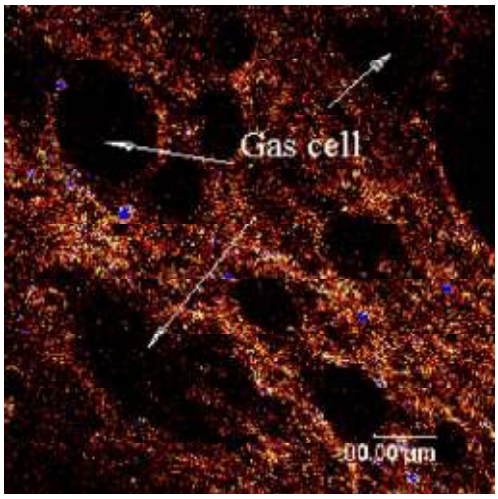

Figure 13. CLSM of control bread dough scanned with an objective16*0.5 IMM PL/PLUOT AR under exciting wave length 568 nm and emission wave length 590 nm (Li et al., 2004).

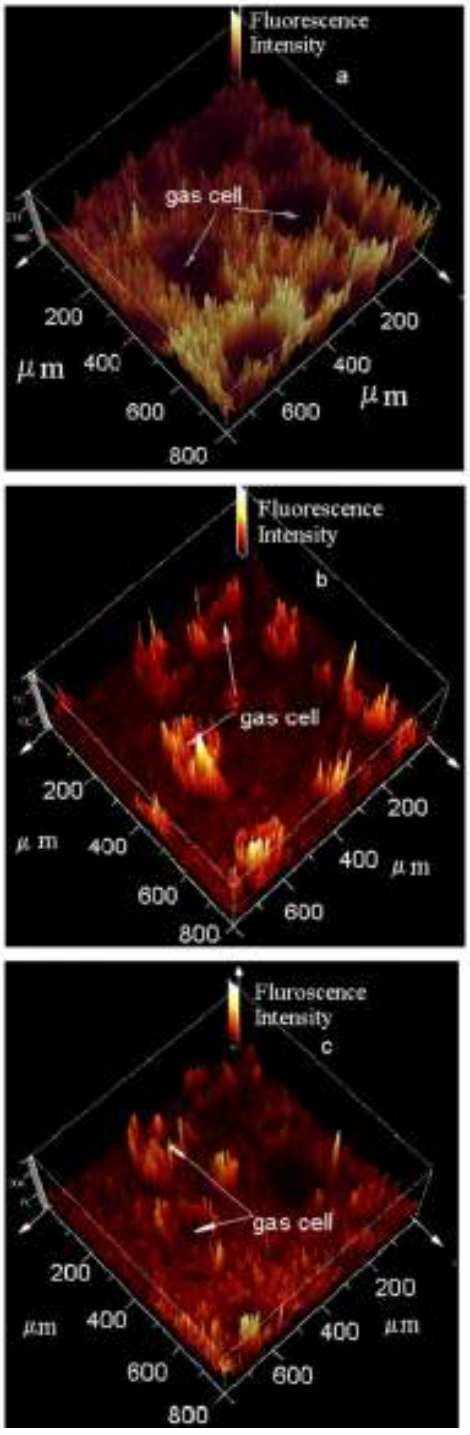

Figure 14. (a)- (c) The fluorescence intensity of gliadin in dough scanned at different depth from the surface of the dough to a depth of 1.2 mm with an objective 16*0.5 IMM PL/PLUOT under wave length 568 and emission wave length 590 nm (Li et al., 2004).

In all previous studies organic dyes such as RhB or FITC were used as a labeling tool to investigate and locate gliadin proteins in the dough matrix. However, one of the main disadvantages of using organic dyes is their higher sensitivity to laser illumination which causes bleaching in time. During imaging of food structure by organic dyes only one fluorescence channel is available which does not allow multiple illuminations (Sozer et al. 2012). Therefore, developments in molecular biology, cell biology and medical immunology have resulted in great improvement in fluorescent labeling techniques which have been used to get a much clearer understanding of how gluten proteins are organized and distributed in dough.

2.9. Quantum Dot Labeling Technique

Quantum dots are tiny particles, or "nanoparticles", of a semiconductor material. They are in the range of 4 to 12 nm in diameter (about the width of 50 atoms). Because of their small size, quantum dots display unique optical and electrical properties. The most immediately apparent of these is the emission of photons under excitation, which are visible to the human eye as light. Moreover, the wavelength of these photon emissions depends not only on the material from which the quantum dot is made, but also to its size. The ability to precisely control the size of a quantum dot enables the manufacturer to determine the wavelength of the emission, which in turn determines the color of light the human eye perceives. Quantum dots can therefore be "tuned" during production to emit any color of light desired. The smaller the dot, the closer it is to the blue end of the spectrum, and the larger the dot, the closer to the red end. Dots can even be tuned beyond visible light, into the infra-red or into the ultra-violet. Figure 15 shows the fluorescence image of CdSe QDs and absorbance spectrum as a function of size (Halpert et al., 2006).

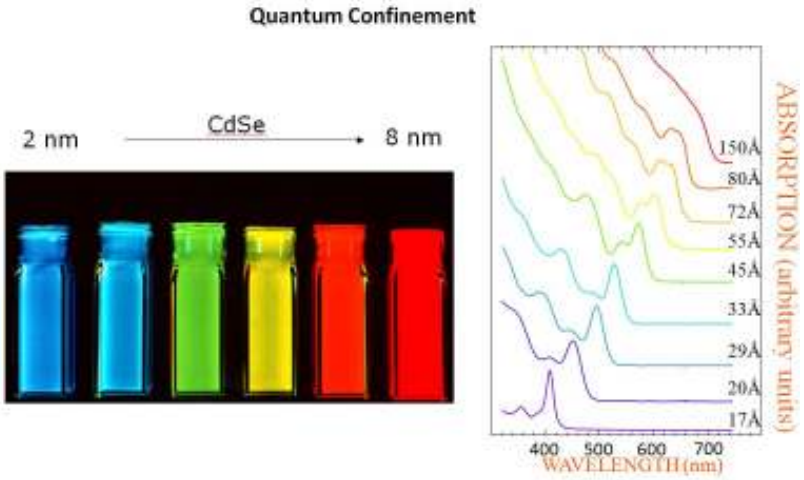

Figure 15. Fluorescence image of CdSe QDs as a function of size (left). Absorbance spectrum as a function of size (right) (Halpert et al., 2006).

2.9.1. Quantum Dots Characteristics

Quantum dots are nanometer sized semiconductor crystals and have recently received a lot of attention due to their unique properties as stable and bright, multicolored fluorescent labeling probes. Currently, the major type of QDs consists of II-IV, IV-IV or III-V (e.g. CdTe, CdSe, PbSe, GaSe, GaN, InP and InAs). Semiconductor core which is coated by a wide bandgap semiconductor shell such as ZnS to minimize the surface deficiency and enhance the quantum yield (Jin et al., 2011). They are inorganic and photochemically robust. Also, the high brightness, long-lasting, size-tunable and narrow, Gaussian emission spectra of QDs that can be excited at a single wavelength, enables multiplex experiments which set them apart from organic dyes (Rosenthal et al., 2010). For instance, the fluorescence intensity of a single CdSe QD is about 20 times higher than an organic dye. However, the most important advantage of using QDs is that different QDs with different emission wavelengths can be stimulated with just one specific excitation wavelength, simultaneously which is very difficult to achieve with organic dyes (Hua et al., 2006).

QDs are hydrophobic and polar QDs need to be created to use in biology. Therefore numerous methods have been developed for creating hydrophilic QDs, which can be divided into two main categories. The first route is commonly designated as “cap exchange”. The hydrophobic layer makes them soluble in non-polar organic solvents. The hydrophobic layer can be coated with or can be replaced with biofunctional molecules containing a soft acidic group (usually a thiol, e.g. sodium thiolycolate) and hydrophilic groups (for example carboxylic or amine groups) which point outwards from the QDs surfaces towards bulk water molecules. The second route is native surface modification, for example, adding of a silica shell to the nanoparticles by using a silica precursor (usually alkoxysilanes such as tetraethylorthosilicate, TEOS) during the polycondensation. Amorphous silica shell can be further functionalized with other molecules or polymers. Another example can be introducing of amphiphilic molecule such as phospholipids. This procedure is preferred for commercially produced biocompatible QDs (Drbohlavova et al., 2009).

QDs were initially considered as potential probes to replace organic fluorophores for biological applications because of their advantageous properties. Researchers have demonstrated the use of QDs for cell labeling, tracking cell migration, pathogen detection, genomic detection, fluorescence resonance energy transfer (FRET) and high-throughput screening of biomolecules Klostranec and Chan, 2006). For instance, the conjugated luminescent QDs to transferring (an ion transport protein) antibodies that recognize cancer biomarkers and folic acid (a small vitamin molecule recognized by many cancer cells) was used by Chan and coworkers (2002) (Figure 16). Also, a further application of QDs is the multiplexed optical encoding and high-throughput analysis of genes and proteins was reported by Han and coworkers (2001). Polystyrene beads are embedded with multicolor CdSe QDs at various color and intensity combinations (Figure 17).

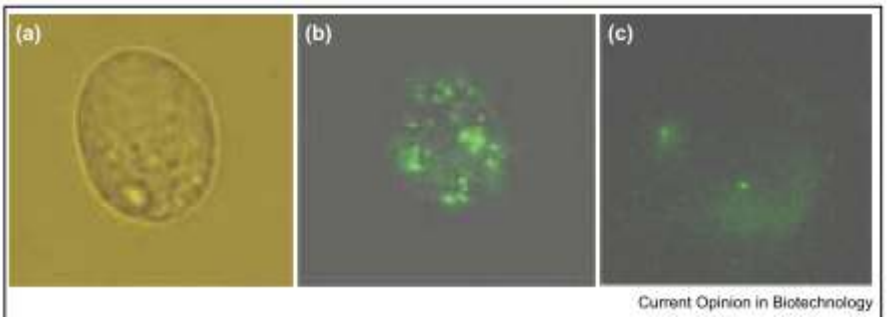

Figure 16. Fluorescence imaging of folate-conjugated QDs inside human cancer cells. (a) Bright-field image of control KB cell (without QDs). (b) KB cell incubated with folate-conjugated QDs. (c) KB cell incubated with bovine serumalbumin-conjugated QDs (Chan et al., 2002).

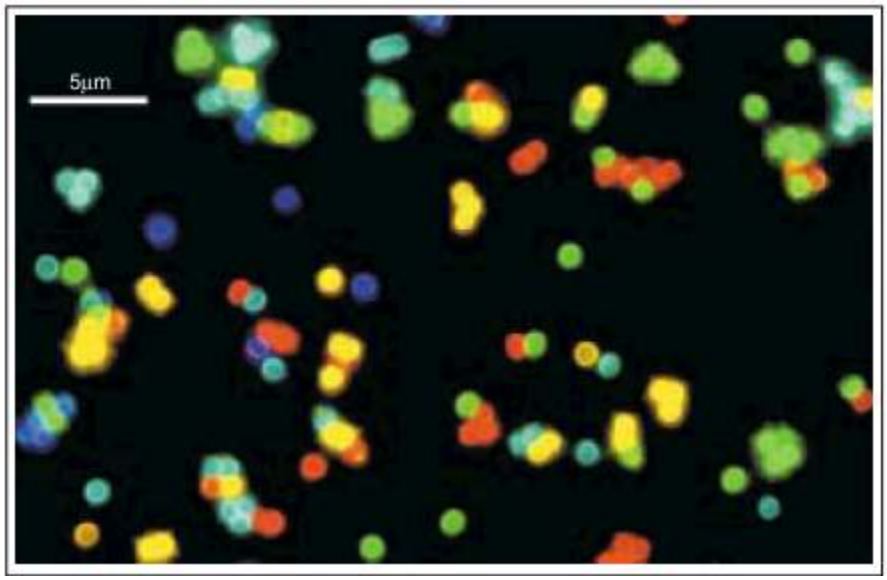

Figure 17. Fluorescence micrograph of a mixture of CdSe/ZnS QD-tagged beads emitting single-color signals at 484, 508, 547, 575, and 611 nm. The beads were spread and immobilized on a polylysine-coated glass slide, which caused a slight clustering effect (Han et al., 2001).

2.9.2. Conjugation

There are many methods for binding biomolecules to QDs including covalent bonding, physical adsorption and hydrophobic adsorption. Covalent attachment of biomolecules to quantum dots is achieved through direct linkage to the quantum dot surface coating or via small molecule cross-linkers. For example, ethyl-3-(dimethyl aminopropyl) carbodiimide (EDC) can be used to couple carboxylic acid-terminated QDs to biologically active molecules containing amine groups. However, crosslinking reagent such as Succinimidyl-4-(N-maleimidomethyl) cyclohexane-1-carboxylate (SMCC) and N-hydroxysuccinimide (NHS) can be used to couple thiols to QDs which have amino functionality on their surface. Covalent attachment is a simple, effective way of linking biomolecules to quantum dots and contributes minimally to the overall bioconjugate size.

Another common conjugation scheme employs the biotin-streptavidin linkage, which requires coupling of the QD to streptavidin. Quantum dot-streptavidin conjugates are useful because a wide range of proteins and other biomolecules can be biotinylated. These conjugates have applications in staining and labeling, live tracking, and drug screening (Walling et al, 2009). Figure 18 shows the various strategies for conjugating biomolecule to QDs (Vashist et al., 2006).

Methods based on electrostatic interactions have also been used for non-covalent biomolecular attachment. For example, quantum dots capped with dihydrolipoic acid (DHLA) can be bound electrostatically to positively charged proteins and have been used in imaging experiments (Jaiswal et al, 2003) or detection assays (Goldman et al, 2004). While electrostatic interactions are less stable than covalent attachment, quantum dot-bioconjugates formed in this way can be used for many of the same applications.

Direct adsorption of a biomolecule to a quantum dot surface is another non-covalent attachment method. Chemically modified peptides and other biomolecules have been shown to adsorb spontaneously on the surface of water-soluble CdSe/ZnS quantum dots (Walling et al, 2009). For example, QDs coated with adsorbed peptides have been used in vivo imaging to locate cells with specific surface proteins (Pinaud et al., 2004).

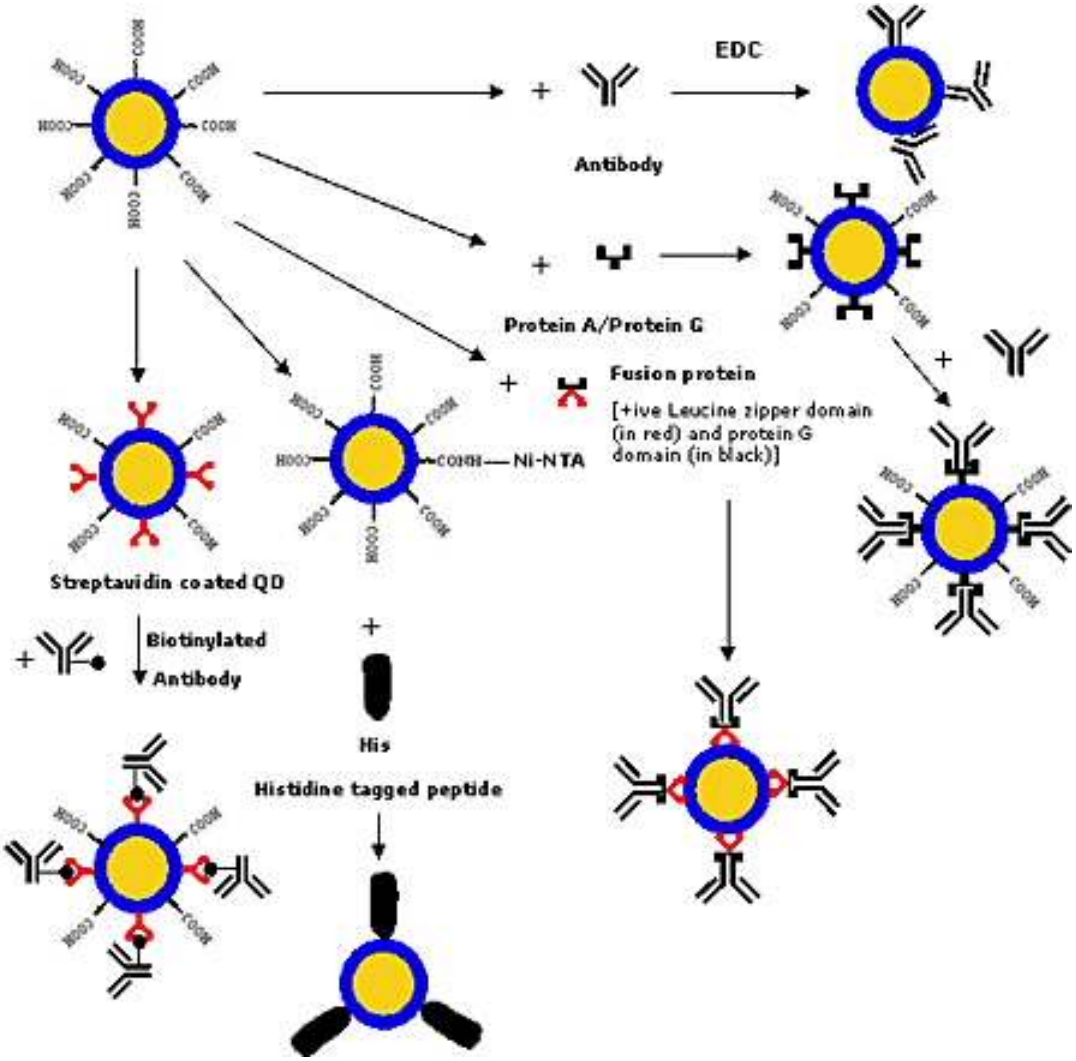

Figure 18. Various strategies for conjugating antibodies/proteins to QDs (Vashist et al., 2006).

2.9.3. Conjugation of QDs to Antibodies

There are three primary ways to conjugate QDs to antibodies. The first one is to label a target directly which might include antibodies, peptides and small molecules. The simplest labeling strategy is using an antibody and the more complicated strategy is using a small molecule. Each approach has its advantages and disadvantages. However, there is no universal approach for all applications. The antibody targeting is described in more details here since in this study where QDs were conjugated with antibody. Figure 19 shows the schematic of QDs conjugation to antibody (Walling et al, 2009).

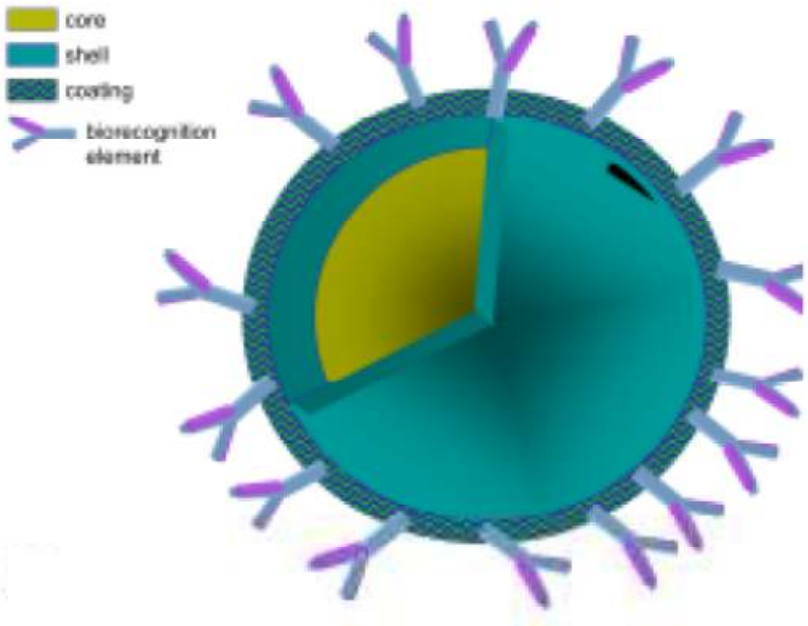

Figure 19. Schematic of QDs-antibody conjugation (Walling et al, 2009).

The simplest and quickest labeling method is to use antibody-QD conjugates, when there is an antibody for an extracellular epitope as a target. Antibody-QD conjugates have been used in various applications. Bentzen et al. (2005) used antibodies for Fusion (F) and attachment (G)

proteins on two sizes of QDs, F protein (605 nm QDs) and G protein (525 nm QDs) to detect and follow the progression of respiratory syncytial viral infection in vitro. The F proteins mediate the fusion of the viral membrane with the host cell membrane delivering the nucleocapsid of the virion particle into the host cell cytoplasm. The G surface glycol proteins aids in attachment of the virion to a host cell.

Gao et al. (2004) used antibody-QD conjugates to target a prostate-specific membrane antigen in tumors in vivo in mice. Also, the use of anti-HER_2 QDs conjugates have been reported in imaging of breast cancer cells in vitro (Wu et al., 2002) and in vivo (Tada et al., 2007). HER_2 (Human Epidermal Growth Factor Receptor 2) is a protein in humans which is encoded by the $ERBB_2$ gene. Amplification or over expression of this gene plays an important role in the pathogenesis and progression of certain aggressive type of breast cancer. It is an important biomarker for breast cancer cell.

Antibodies can be biotinylated and used with streptavidin-coated QDs or they can be directly conjugated to QDs. Wide selections of antibody-QD conjugates are also commercially available. However, the availability of antibodies, the challenges that one faces with their selectivity and affinity are the disadvantages of this method.

Understanding the molecular mechanisms of protein binding, signaling and regulation have been a long term goal for cell biology. Using QDs as a fluorescent tag for single protein tracking is a revolutionary tool in life science research. Dahan and et al., (2003) performed the first single protein tracking with QDs probes. They tracked the diffusion of individual glycin receptors with antibody-QD conjugates in living neuronal cells. They used a primary antibody (mAb2b), biotinylated anti-mouse Fab fragments and streptavidin coated QDs (Figure 20). Cui et

al. (2007) labeled the biotinylated nerve growth factor (NGF) signals with streptavidin-conjugated QDs to track the movement of NGF in live neurons in real time.

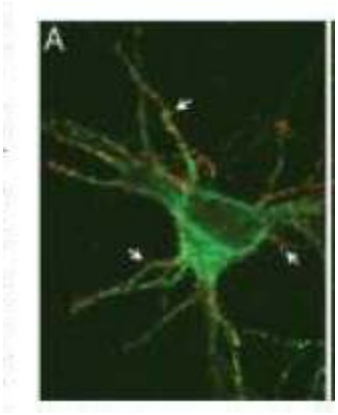

Figure 20. QDs as a marker for GlyR localization in neurons. Arrow: mark clusters of QD-GlyRs located on dendrites (Dahan et al., 2003).

2.9.4. QDs Applications

The utility of quantum dots has been demonstrated in a variety of biological and clinical applications, such as immunohistochemical detection, drug delivery and therapeutics, biosensing, small animal imaging and single-quantum dot tracking of extra and intracellular targets (Medintz et al., 2008; Delehanty et al., 2009; Medintz and Mattoussi, 2009; Gao et al., 2004; Pinaud et al., 2010; Rosenthal et al., 2011). Figure 21 shows some examples of QDs bioanalytical and biomedical applications (Drbohlavova et al, 2009).

Since QDs have unique physical and optical properties and the possibility of being conjugated to various biomolecule surfaces, they are very effective in biosensing applications. For example, the detection of adenosine-triphosphate (ATP) using a QD tagged nucleic acid that binds to molecular targets such as thrombin, adenosine or cocaine was described by Chen et al., (2006). They used 605 QDs as donor and organic fluorophore (Cy5) as acceptor to detect ATP.

There are several possibilities for using QDs in biolabeling and cellular imaging both in vitro and in vivo. The biological applications of QDs are described in more details in the next section.

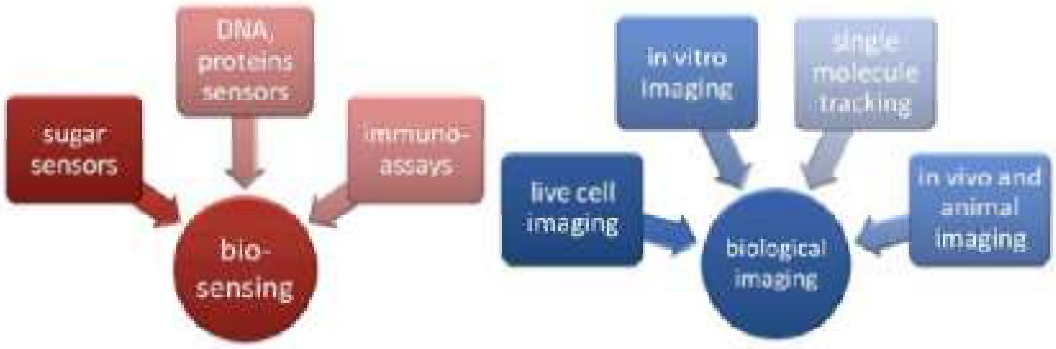

Figure 21. QDs bioanalytical and biomedical applications (Drbohlavova et al., 2009).

2.9.4.1. FRET and Gene Technology

Fluorescence resonance energy transfer (FRTE) is a useful method for measuring and characterizing protein conformational changes, monitoring protein interactions and assaying enzyme activity. Several groups used QDs in FRTE technology, particularly when conjugated to biological molecules including antibodies for use in immunoassay (Jamieson et al., 2007). Willard et al. (2001) demonstrated a biotin-streptavidin binding assay wherein specific binding of tetramethylrhodamine labeled streptavidin (SAV-TMR) to biotinylated bovine serum albumin (bBSA) conjugated to CdSe-ZnS QDs (Qd-bBSA) was observed via enhancement of the TMR fluorescence due to FRTE from the QD donors to the TMR acceptors (Figure 22).

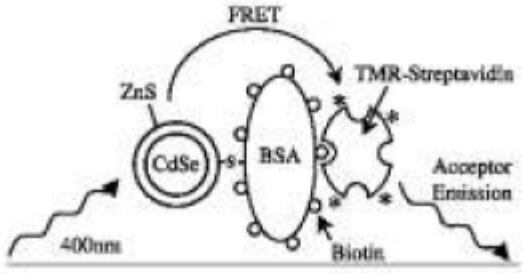

Figure 22. Schematic of FRET binding assay (Willard et al., 2001).

In regard to applications of QDs in gene technology, a number of studies have shown that QD-conjugated oligonucleotide sequences may be targeted to bind with DNA or mRNA (Pathak et al., 2001 and Gerion et al., 2002). Also, using red, green and blue QDs in a number of combinations, the specific labeling and identification of target sequences of DNA has been demonstrated (Figure 23) (Han et al, 2001).

QD-FRTE has also been used in genetic applications for determining the dynamics of telomerisation and DNA replications (Patolsky et al., 2003). In addition to use QDs in DNA technology, they may find use in detection of mRNA molecules (Chan et al., 2005).

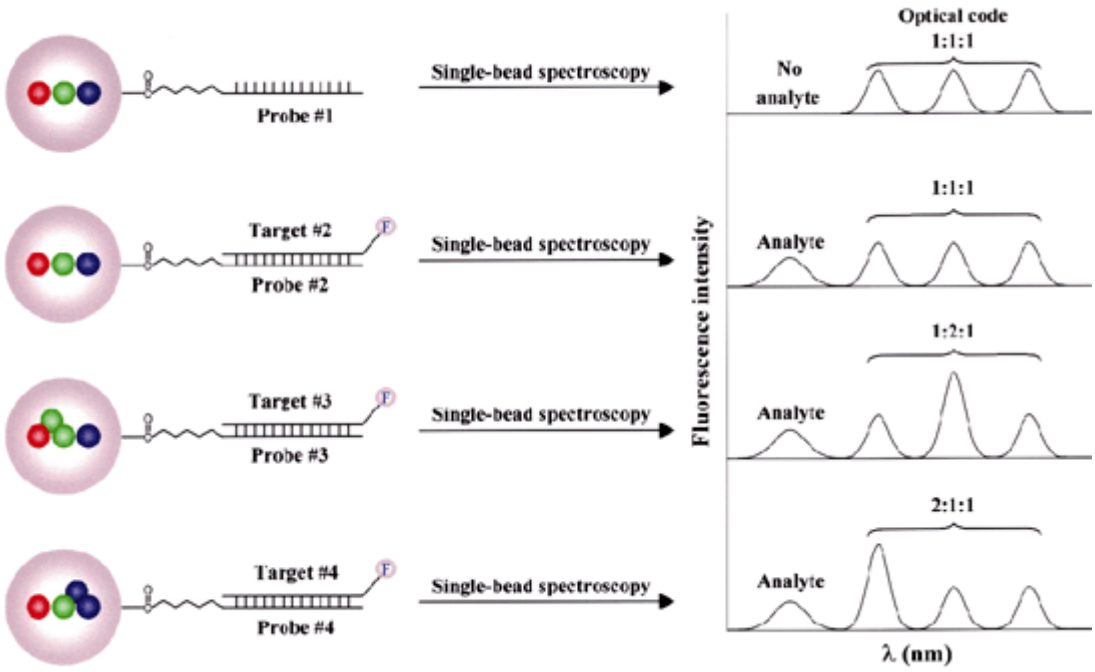

Figure 23. Schematic illustration of DNA hybridization assay using QD-tagged beads (Han et al., 2001).

2.9.4.2. Fluorescent Labeling of Cellular Proteins

External labeling of cells with QDs is relatively simple but intracellular delivery is difficult. Several methods have been used to deliver QDs to the cytoplasm for staining of intracellular structures, but so far these have not been particularly successful. Labeling of F-actin fibers with QDs has been used to label proteins where preservation of enzyme activity was desirable. Figure 24 shows streptavidin- coated QDs that were used to label individual isolated biotinylated F-actin fibers (Wu et al., 2003).

Cellular labeling with QDs has made the most progress and attracted the greatest interest. A number of groups reported multiple colors labeling of different intracellular structures (Hanaki et al., 2003 and Hoshino et al., 2004). QDs labeling permits extended visualization of cells

under continues illumination as well as multicolor imaging of different proteins and cellular structures and highlighted the advantages offered by these fluorophores. Figure 25 shows pseudocolored image of five-color QDs staining of fixed human epithelial cells. In this image nucleus, Ki-67 protein, mitochondria, microtubules and actin filaments were labeled with five different QDs, simultaneously (Medintz et al., 2005).

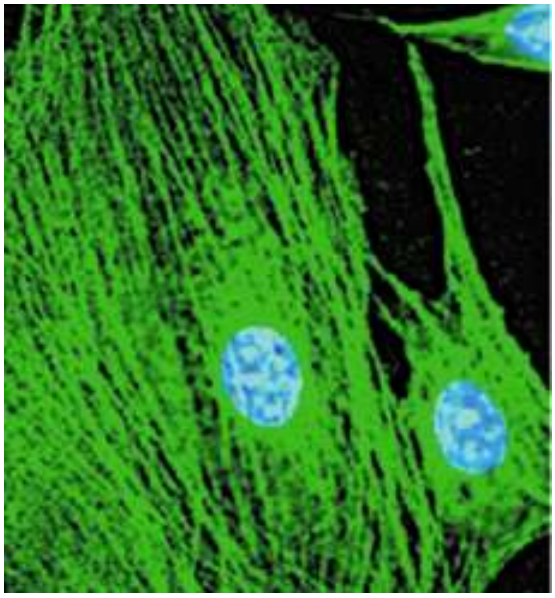

Figure 24. Actin filaments stained with biotinylated phalloidin and QD 535–streptavidin, and nuclei counterstained with Hoechst 33342 blue dye in mouse 3T3 fibroblasts (Wu et al., 2003).

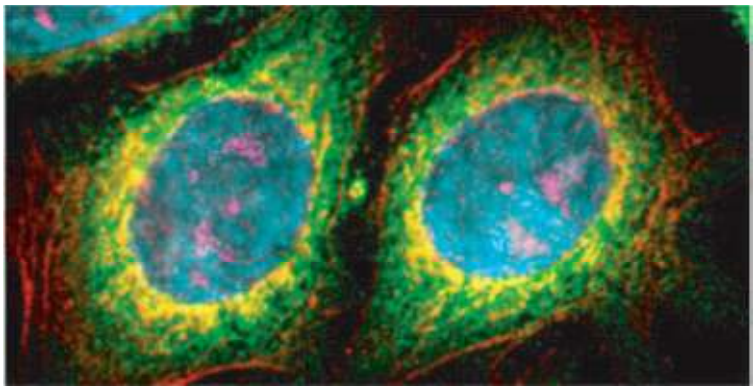

Figure 25. Pseudocoloured image depicting five-color QD staining of fixed human epithelial cells. Cyan corresponds to 655-nm Qdots labeling the nucleus, magenta 605-Qdots labeling Ki-67 protein, orange 525-Qdots labeling mitochondria, green 565-Qdots labeling microtubules and red 705-Qdots labeling actin filaments (Medintz et al, 2005).

2.9.4.3. Pathogen and Toxin Detection

QDs may find practical application for the detection of pathogens and toxins. A number of studies have reported good results and the opportunity for multiplex imaging to detect pathogens and toxins. For example, labeling of both *C. parvum* and *G. lamblia* using immunofluorescent staining methods with QD fluorophores was reported (Zhu et al., 2004). QDs conjugated to wheat germ agglutinin and transferrin have been used to label both bacterial and fungal populations (Kloepfer et al., 2003). CdTe QDs capped with mercaptopropionic acid (3-MPA) were used as an imaging tool to label Salmonella typhimurium cells (Li et al., 2007). A number of studies also have used QDs for detection of toxins (Goldman et al., 2002 and Goldman et al., 2004). Goldman et al. (2004) demonstrated the simultaneous detection of the four toxins (cholera toxin, ricin, shiga-like toxin and staphylococcal exterotoxinB) from a single sample probed with a mixture of all four QDs-antibody regents.

2.9.4.4. Cell Tracking

QDs can also be used in cell tracking by using avidin-conjugated QDs to label cells. With the development of biomarkers in cell biology, the tracking of some specific cells such as cancer cells becomes possible (Jin et al., 2011). There are important studies on the tracking and diagnostic of cancer cells with QDs. Near-infrared (near-ir) quantum dots (QDs) are well known for their excellent optical characteristics. They hold great potential for applications in non-invasive long term observation and tracing of cells in vivo. Cancer specific antibody, coupled to near-IR QDs with polymer coating is the most popular QDs agent for tumor targeted imaging.

Cao et al. (2010) uses near-IR QDs with emission wavelength 800 nm to label squamous cell carcinoma cell line U14. The recently developed near-ir QDs with an emission wavelength range from 700 to 900 nm not only have strong penetration in human tissue but can also avoid the interference of tissue autofluorescence (emission range from 400 to 600 nm).Thus they are particularly suitable for in vivo non-invasive medical imaging The fluorescent images of U14 cells after 6 hours were obtained by cell endocytosis (Figure 26) (Cao et al., 2010).

Other types of QDs which have been used in pancreatic cell imaging include CsSe/CdS/ZnS QDs using transferrin and anti-Claudin-4 as targeting ligands (Qian et al., 2007 and Erogbogo et al., 2008). Yong et al. (2009) reported CdSe/CdS/ ZnS QDs coated with PEG phospholipids and RGD peptide for tumor targeting. It was demonstrated that this conjugation method gave bright, photostable and biocompatible luminescent probe for early diagnosis of cancer and it was a new opportunity for imaging early tumor growth.

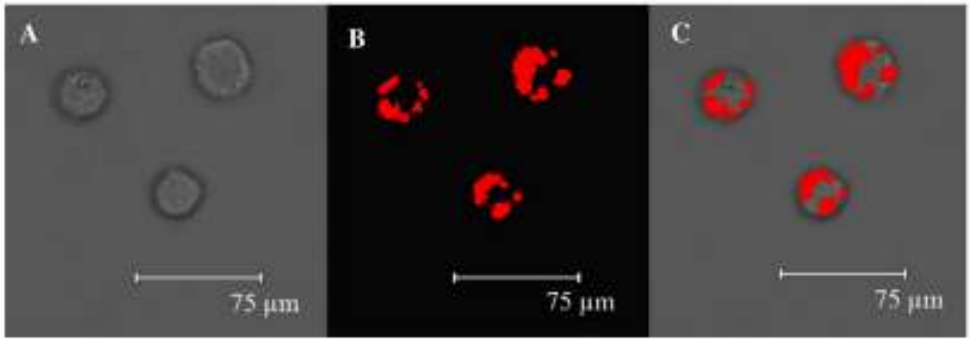

Figure 26. Fluorescent images of U14 cells 6h after labeling with QD80.(A) Bright light. (B) QD80 fluoresence image and (C) overlay image (Cao et al., 2010).

2.9.4.5. In Vivo Imaging

In addition to QDs' use as nanoprobes and labels for in vitro imaging, QDs have also been widely used for in vivo imaging (Xing et al., 2009). QDs have been used for non-targeted imaging in various animal models. Ballou and coworkers (2004) injected PEG-coated QDs into mouse blood stream and investigated the effect of surface coating on circulation lifetime.

Larson and coworkers (2003) injected green QDs 550 nm in a living mouse and visualized them through the skin (Figure 27). For the first time, Akerman and coworkers (2002) explored the possibilities of using QD-peptide conjugates to target tumor vasculatures in vivo. QDs coated with peptides targeting the lung vasculature, blood vessel and tumor cell or lymphatic vessels were injected systematically into mouse. Figure 28 shows images of QD tagged prostate specific membrane antigen (PSMA) antibodies at the tumor site in vivo (Gao et al., 2004).

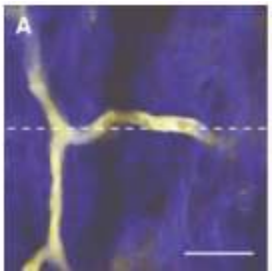

Figure 27. In vivo imaging of vasculature labeled by a tail vein injection of Qds, 550 nm (Larson et al., 2003).

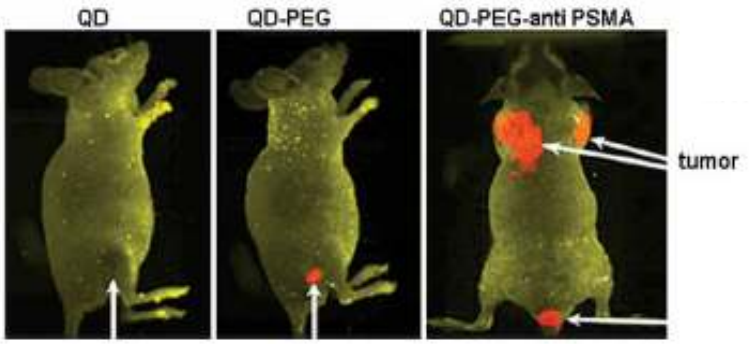

Figure 28. Targeted tumor imaging using QD antibody conjugates (Gao et al., 2004).

2.10. Quantum Dots Application in Food Science

Nowadays quantum dots technology is most commonly used in variety of bioanalytical and biomedical applications based on their unique physical and optical properties and the possibility of attaching to various biomoleclues. Also, the application of this technology could have a lot of impacts in food science. For instance, they can be used as anti-fraud tools when they are printed as codes or patterns on food and beverage labels which can be visualized by a specific light source. This application of QDs in food packaging can help to follow the

fingerprints of the food product. Another novel perspective for the application of QDs in food science can be using them as fluorescence probes.

Sozer et al. (2012) used carboxy activated QDs as a fluorescence probe to tag and track gluten proteins in bread samples. They compared the benefit of using QDs as a probe with organic dye (Rhodamine B) in imaging of protein matrices in flat bread samples. Their result showed that QDs can be a good alternative against organic dyes and they were better probes for imaging in comparison to Rhodamine B.

In this study, we used this novel perspective of QDs application as a fluorescence probe to track the distribution of gluten subfraction (i.e., gliadin proteins) in dough and flat bread and the effect of heat on its distribution. For determination of gliadin proteins, a gliadin antibody, which is specifically bond to gliadin, was used. Therefore, QDs was conjugated to gliadin antibody and used as a labeling tool to monitor the distribution of gliadin proteins in different samples. Confocal laser scanning microscopy was used for imaging of conjugated QDs-gliadin antibody and the numerical intensity values were obtained through image analysis software program.

Chapter Three:

Materials and Methods

3.1. Materials

Wheat flour, enriched and bleached, (Gold Medalbrand, manufactured by General Mills, Minneapolis, MN) needed to prepare bread sample was purchased from a supermarket. The approximate protein content was 10.5%, carbohydrate content was 79.3%, dietary fiber was about 3.5 % and the fat content was negligible.

Commercially available, native and heat-treated polyclonal gliadin antibody was purchased from Sigma-Aldrich, St Louis, Mo. Quantum dots with a CdSe core coated with ZnS and polyethylene glycol (PEG) approximately in the range of 15 to 20 nm in size were purchased from Invitrogen, Carlsbad, CA. in the form of a kit (Qdot-625 antibody conjugation kit). The quantum dots were amine activated for crosslinking to enable conjugation with gliadin antibody.

PBS buffer concentrate was purchased from Sigma Aldrich and was diluted 10 times to reach the pH of the phosphate buffer saline solution.The hydrophobic positively charged microscope slides were obtained from Fisher Scientific through the Institute of Genomic Biology of the U of I and were used to appropriately fix the sample on them for CLSM studies .

3.2. Methods

3.2.1. Preparation of Samples

3.2.1.1. Preparation of Wheat Flour Dough

Dough sample was prepared by hand mixing of 50 g of wheat flour with 32 mL of distilled water. This water content was that needed to reach a 500 BU value with a Farinogram. The dough sample was hand kneaded and shaped into a ball, pressing it down and reshaping it

continuously for 5 minutes. Then, the dough was allowed to rise for 5 minutes at room temperature in a wrapped plastic. (Sozer and Kokini, 2013). After the sample went through all these preparation steps 57 g of dough was weighed. Flour was sprinkled over the dry flat surface to prevent the dough from becoming sticky. Then the dough was sheeted on a flat surface using a rolling pin in all directions until the thickness of dough became 1.87mm. The thickness of the dough was measured using a caliper.

A circular 4 inch cutting die was used to cut the dough with an accurate diameter with a thickness of 1.87mm. Then the dough sample was stored in a closed glass plate in a freezer at a -20°C temperature. Figure 1 shows an example of the dough sample.

Figure 29. dough sample.

3.2.1.2. Preparation of Flat Bread

Flat bread samples were prepared by making dough as described in the previous steps. Once the thickness of dough reached 1.87 mm, it was cooked at oven temperature of 375°F for two different baking times of 5 minutes and 9 minutes. The samples were then allowed to equilibrate at room temperature and 5mmX5mm square pieces were cut from the baked bread for QD antibody conjugation in a procedure described below.

3.2.2. Conjugation of Gliadin Antibody to Quantum Dots

Conjugation of gliadin antibody to quantum dots (QDs) was conducted based on the protocol which Invitrogen Company provided. The QDs antibody conjugation kit contains 4 μM amin-derivatized, PEG-coated QDs, 10 mM solution amine-thiol crosslinker SMCC (Succinimidyl-4-(N-maleimidomethyl) cyclohexane-1-carboxylat) which allow us to conjugate to gliadin antibody, 1M DDT solution, 14.3 M 2-mercaptoethanol, desalting column, column for separation of media, and centrifugation tube. Two separate conjugation reaction of QDs nanocrystal to an antibody sample was performed. The conjugation reaction can be completed based on the fast and efficient coupling of thiols that are present in reduced antibodies to reactive maleimide groups present on the nanocrystal after SMCC activation. The protocol contains 11 steps: 1. Preparing for the conjugation reaction, 2. Activating QDs nanocrystal, 3. Reducing the antibody sample, 4. Equilibrating the desalting column, 5. Desalting and collecting reduced antibody, 6. Desalting and collecting the activated QDs nanocrystal, 7. Conjugation reaction, 8. Quenching the conjugation reaction, 9. Preparing the separation column, and 10. Concentrating the sample, 11. Separating the conjugated antibody from unconjugated antibody. Figure 30 shows the diagram of Qds antibody conjugation procedure.

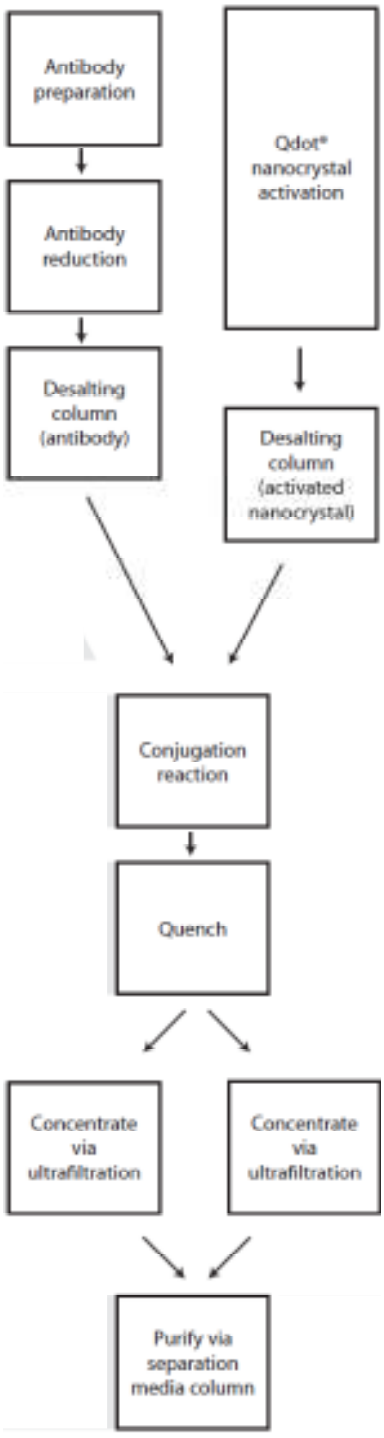

Figure 30. Diagram of the QD antibody conjugation procedure (Invitrogen Co.).

In first step, SMCC solution was thawed at 37°C for at least 15 minutes before use. 300 µL of a 1 mg/mL antibody solution was prepared in PBS. For activation QD nanocrystals, 125 µL of QDs was added to the tube containing the SMCC and vortex briefly to mix. Incubate for 1 h at room temperature to active the nanocrystals. 6.1 microliters of 1 M dithiothreitol (DTT) as a strong reductive reagent was added to 300 microliters of antibody to reduce the antibody solution and mix and incubated for 30 minutes at room temperature. Two desalting columns were used to "reduce antibody" and the other to "activate QD" nanocrystals. Each column gel was equilibrated with exchange buffer (50 mM MES, 2 mM EDTA, pH 6.0). After entering exchange buffer to gel bed of column, reduced antibody mixture was added to the top of the gel bed. 500 µL of the reduced antibody solution was collected (the maximum collection was 500 µL because higher volumes may contain residual DDT that interferes with the conjugation) into a centrifugation tube. For the desalting column labeled with "activated QDs" the same procedure which was done for "reduced antibody" was followed. In the conjugation step, the reduced antibody and activated QDs were reacted for 1 h at room temperature. To quench the conjugation reaction, 2-mercaptoethanol was added to the reaction medium. The incubation time was 30 minutes at room temperature. The quenched conjugation reaction was divided into two ultrafiltration devices. Each reaction was concentrated to 20 µL by centrifuging at 4000 * g for approximately 20 minutes. The conjugated antibody was separated from unconjugated antibody in a separation column.

QDs were conjugated to gliadin antibody through covalent linkage in presence of SMCC (Succinimidyl-4-(N-maleimidomethyl) cyclohexane-1-carboxylat) cross linker. Based on the protocol, first the QDs nanocrystal was activated by mixing of QDs nanocrystal with SMCC solution and incubated for 1 hour. Second, the gliadin antibody is reduced by using 1M DTT

solution. An antibody or also known as an immunoglobulin (Ig) is a large Y-shaped protein and basically contains two heavy chains and two light chains. The heavy and light chains and two heavy chains are held together by inter-chain disulfide (S-S) bonds. Also, there are intramolecular disulfide S-S bonds within each of the polypeptide chains. In order to have a reaction between the gliadin antibody and QDs-SMCC,the gliadin antibody should be reduced. DTT reduces the inter-chain S-S bonds of the antibody to free S-H groups for reaction with QDs-SMCC. SMCC is a popular cross linker that has an amine-reactive NHS-ester group at one end which reacts with QDs and a sulfhydryl reactive maleimide group which reacts with anti-gliadin antibody. This allows for sequential, two-step conjugation procedures. The schematic reaction of SMCC cross linker is shown in Figure 31.

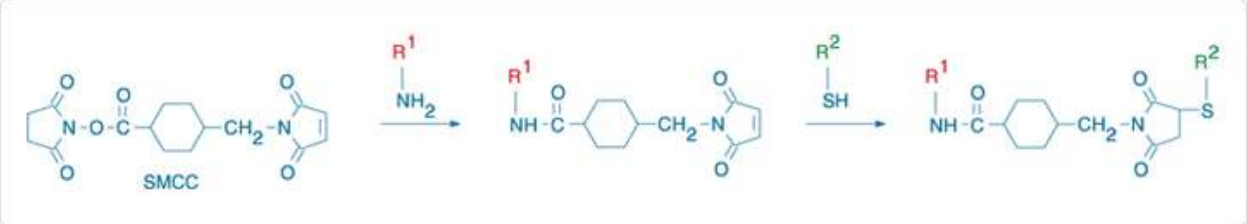

Figure 31. The schematic reaction of SMCC cross linker. Amine-reactive NHS-ester group at left and sulfhydryl reactive maleimide group at right.

After conjugation of QDs to gliadin antibody, the quenching of the conjugation reaction was conducted in the presence of 2-mercaptoethanol for 30 minutes at room temperature. Since 2-mercaptoethanol has S-H group, it can be used to deactivate any unreacted QDs. A separation media was used for preparing the separation cloumn. The separation media is supplied as a suspension containing 20% ethanol as a preservative. It should be a uniform suspension before loading into column. The column begins to drip at the bottom after loading the meadia into it.

We then added 0.5 mL distilled water to top the gel. The column was filled with PBS pH 7.2 solution when the solvent level drops to near the top of the settled gel bed. PBS was drawn by syringue to just above the top of the gel bed. This PBS fill and drain was repeated two more times until the PBS was 2 to 3 mm above the top of the settled gel bed line. The syringue was removed and the bottom and top caps was replaced. At this time the separation column is ready.

For separation the conjugated antibody from unconjugated antibody, the separation column was uncapped and eluted with PBS solution and then the column was filled with the sample to elute by gravity. Two different orange and pink colors can be observed in the column. The pink color comes from the dye marker added to the gliadin antibody reduction reaction and the orange color comes from conjugated and unconjugated gliadin antibody. However, the first 10 drops have more orange color and come from conjugated gliadin antibody which should be collected in the centrifuge tube. Subsequent drops contain unconjugated gliadin antibody that will interefre with the application of conjugate and should not be collected. Figure 32 shows the separation of conjugated gliadin antibody from unconjugated gliadin antibody.

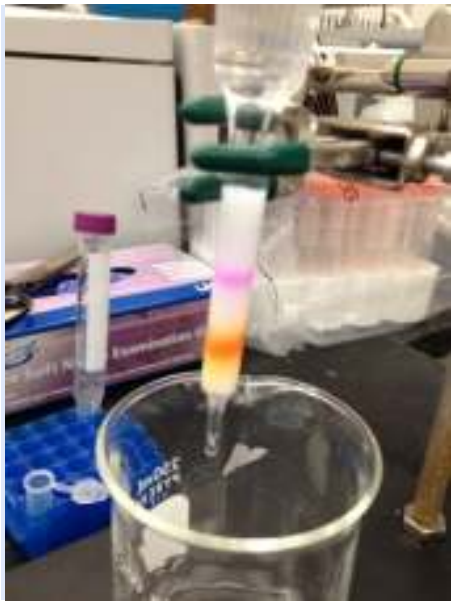

Figure 32. Separation of conjugated gliadin antibody from unconjugated gliadin antibody.

The concentration of the collected conjugated QDs gliadin antibody was determined by measuring the optical density at a wavelength of 625 nm by using the formula $A=\varepsilon cL$, where A is the absorbance, ε is the molar extinction coefficient, c is the molar concentration and L is the path length. The absorbance of the sample in the cuvette with 1 a cm path length and with the QDs extinction coefficient of 500000 $M^{-1}cm^{-1}$ at 625 nm was 0.66 μM cm. Based on the formula $A=\varepsilon cL$, the molar concentration of QDs gliadin antibody was 1.32 μM. The conjugate was stored at 4°C in refrigerator.

3.2.3. Sectioning of Samples for Microscopy Imaging

In order to obtain the distribution of gliadin throughout the sample, each sample was cut into 4 sections and from each section approximately 5 mm square pieces were cut from the center of the sample. Two different baked bread samples (i.e. backed bread at 5 minutes and backed bread at 9 minutes) were cut using a razor blade as longitudinal sections of top, center

and bottom. Figure 33 shows the three different layers of baked bread. The QDs conjugated with gliadin antibody was diluted with PBS buffer in the ratio of 1/10 (i.e. one microliter QD-antigliadin is diluted in 10 microliter PBS). 5 µL of this diluted QD-anti-gliadin was pipetted on microscope slides. Then the sample was placed on this conjugate solution for imaging with confocal laser scanning microscopy (CLSM). For instance, in order to obtain the microscopy image of the top layer of baked bread at 9 minutes, the face of the top layer was placed on the 5 µL of conjugate solution which is pipetted on the microscope slide. 5 µL of conjugation solution was used to cover all samples on the microscopic slide with solution.

3.2.4. Confocal Laser Scanning Microscopy

The confocal laser scanning microscope (Zeiss LSM 700, Carl Zeiss Microimaging GmbH, Germany) was used. This confocal microscope is based on an Axio Imager upright microscope with an AxioCam digital microscope camera with a Diode laser. The excitation wavelength of the laser was 405 nm and to avoid the autofluorescence of QDs, the reflection wavelength was adjusted between 592-740 nm. A Carl Zeiss objective Plan-Apochromat 20X/0.8 M27 was used. Digital image files with a resolution of 1024X1024 pixels were recorded with the Zen LSM software (Carl Zeiss Microimaging GmbH, Germany) as stacks with the constant z-position. The samples were loaded on a motorized xy stage. For each sample nine images at the same constant distance from nine different regions were taken by LSM 700. The most important criteria for using CLSM is choosing the accurate settings of the detector gain and laser power by avoiding under-saturation and/or over saturation of images.

In this study, to avoid of under-saturation and/or over saturation of images and based on intensity level of QDs-anti-gliadin , the laser power for dough, top and center layer of baked

bread at 9 minutes and top layer of baked bread at 5 minutes was selected at 1.8 %. The laser power for bottom layer of baked bread at 9 minutes and center and bottom layer of baked bread at 5 minutes was selected at 2.8 %. Setting up the CLSM at lower laser power means the sample has higher intensity level of QDs-anti-gliadin. However, the mean intensity for all samples was calculated at the constant laser power 1.8 %.

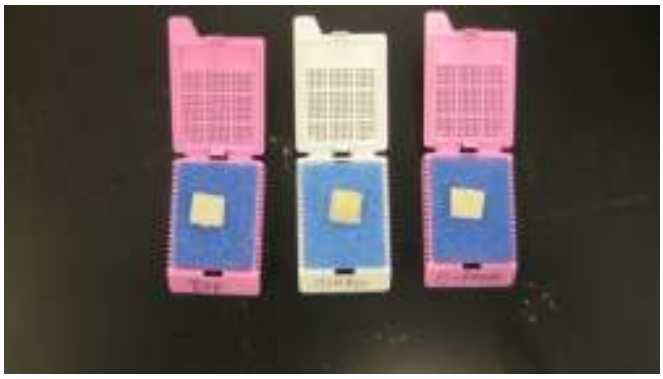

Figure 33. Three layers from left to right top, center and bottom of baked bread samples.

3.2.5. Calculation of Intensity Values from CLSM Images

In confocal laser scanning microscopy the light intensity of the image is detected by a photomultiplier tube (PMT) after passing through a pinhole. The pinhole in CLSM improves the quality of images by avoiding the majority of the light to be reflected and enables to obtain images at various depths in a pre-determined z-stack image. In order to take nine images, the motorized xy stage was moved at nine different regions of sample with the same constant distance, manually. First, the laser power was adjusted on the center of the sample and then the xy stage was moved to right and left at the same distance in each direction to take images in nine different regions. Figure 34 represents the process of sample preparation for microscopy scanning.

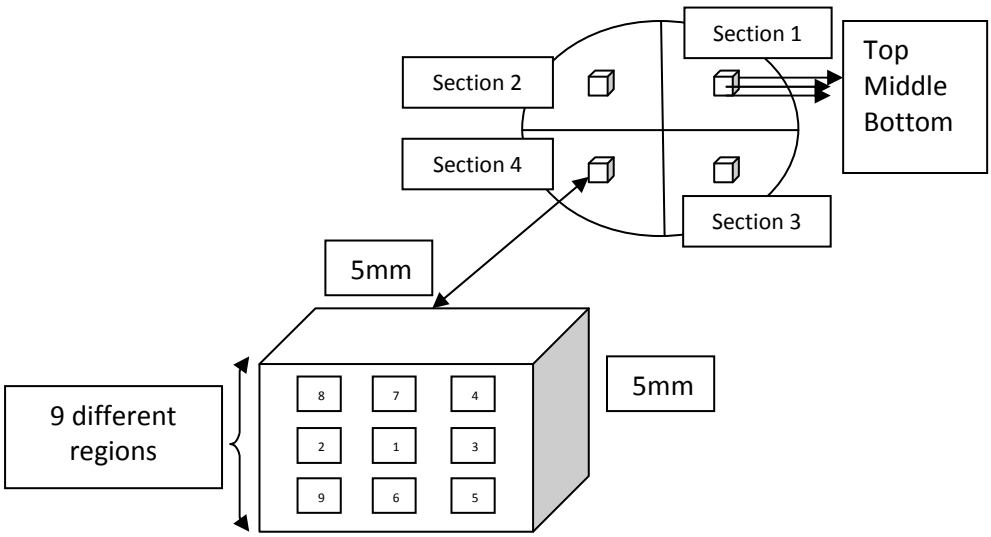

Figure 34. Sample preparation for microscopy scanning.

Each sample was scanned in tile scan mode 2*2 and z-stack of 8 slices to obtain a whole scanned area of target sample. The image is created pixel by pixel and then line by line. Therefore, the brightness of a sample image pixel represents the relative intensity of the detected light which in turn is related to the concentration of gliadin antibody conjugated quantum dots.

In order to do the interactive measurement on each image, Axiovision software (Zeiss, Jena, Germany) was applied. Representative area for intensity from each image was chosen manually and it was constant for all images. Then the sum of intensity values for each image was calculated by adding all relative intensity values for each image. Since for each sample there are four sections and for each section, nine images were taken, the total number of sum intensity values for all images in each sample is equal to 36. The mean intensity values and standard deviation for each sample were calculated by taking an average from sum intensity values.

To consider whether the differences in the distribution of gliadin protein are statistically significant in different samples and different regions, analysis of variance (ANOVA) of the data

was conducted. The ANOVA test was performed using the target significance level $\alpha=0.05$ and $\alpha=0.01$. If the probability (p-value) is less than a significance level (α) this justifies the rejection of the null hypothesis. Rejecting the null hypothesis implies that different treatments result in significantly different fluorescence intensities. In contrast, if the p-value is greater than a significance level (α) this indicates the acceptance of the null hypothesis. This result suggests that fluorescence intensities are not statistically significantly different. The ANOVA with single factor was performed between dough and baked bread at two different baking times to investigate the effect of different samples on distribution of gliadin. Also, the ANOVA test to consider the effect of different sections and specific section in each sample was conducted between two by two different sections in each sample and each four sections in different layers of baked breads at 9 minutes and 5 minutes, separately.

Chapter Four:

Result and Discussion

4.1. CLSM Images of QDs-Anti-Gliadin Conjugate

4.1.1. Variability in the CLSM Image Fluorescence Data

The first important aspect of this work is to recognize that there is a considerable amount of local variation in the fluorescence data obtained after QDots are conjugated with gliadin. First the dough has been mixed by hand and we expect to have local variability in the distribution of the protein network. Second we are working with a biological material with inherent variability and third we expect to have some of the epitopes non-functional because of denaturation of gliadin with heat and also for some of the gliadin to be buried in the glutenin matrix making them inaccessible to gliadin antibodies. We illustrate this variability in Figure 35 by showing two samples the first one consisting of the dough (35A) and the second one the flat bread baked at 9 minutes (35B). These two examples in regions that are very close to one another show how variable the concentration of gliadin and the fluorescence response can be. In order to increase the reliability of the results we will show our ANOVA results later.

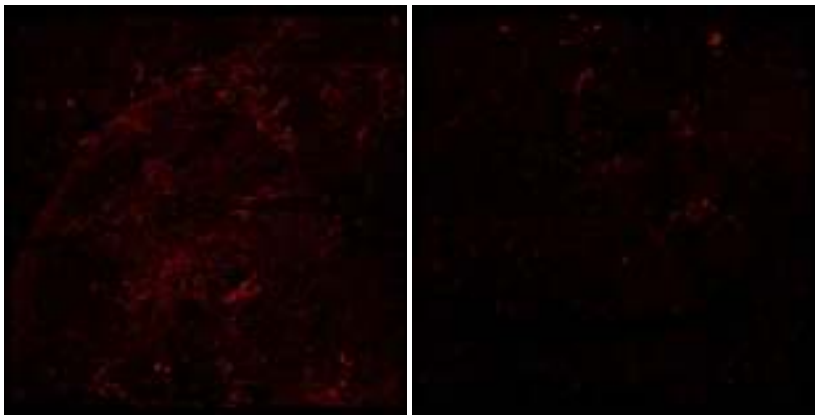

a b

Figure 35 A. Sample 3-D fluorescence intensity profile of QDs-gliadin antibody conjugated images of dough sample for selected image 400 μm x 400 μm in size in different regions at Section 2 of a) Region 5 b) Region 9.

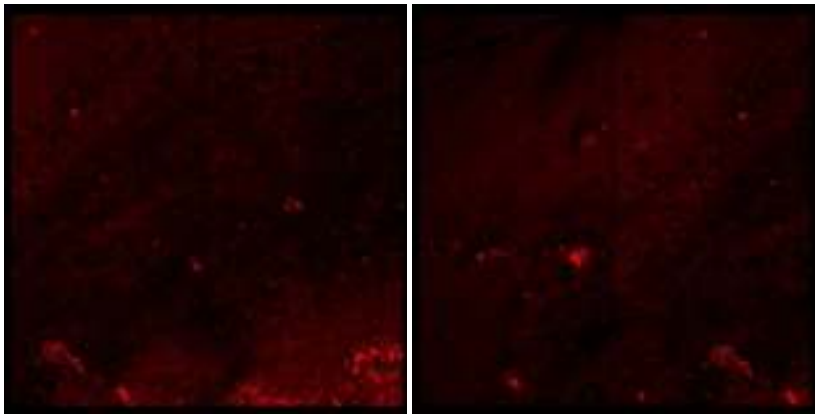

a b

Figure 35 B. Sample 3-D fluorescence intensity profile of QDs-gliadin antibody conjugated images of top layer of bread at 9 min image 400 μmx 400 μm in size in different regions at Section 3 of a) Region 5 b) Region 6.

4.1.2. Distribution of Gliadin in Dough and Baked Bread Based on QD CLSM Fluorescence Data

As described on the Materials and Methods section each sample was divided into four different sections and 9 images were taken from 9 different regions from each section leading to a total number of 36 images for each sample. To calculate the aggregate intensity value for all images the Axiovision software was used. CLSM images of fluorescence intensity generated by QDs-gliadin antibody conjugate for top, center and bottom layers of baked bread sample at 9 minutes baking time are shown in Figure 36. We can see stronger fluorescence intensity in the top layer (layer farthest from direct heat) indicating the presence of more gliadin than what is observed in the center layer and the center layer has more gliadin than the bottom layer (the layer which is closest to direct heat). This clearly shows that the distribution of gliadin protein is not uniform in the 3 different layers of the bread sample baked for 9 minutes. Also, it shows the impact of baking on the distribution of gliadin

Different sections also show varying levels of gliadin in the sample. For example, Figure 37 shows the uncooked dough in sections 3 and 4 as described in methods. These two sections contain different amounts of gliadin protein. Section 3 shows a greater amount of gliadin than section 4 which is confirmed by sum intensity values in Table 2. The mean intensity value of gliadin for all samples was calculated and plotted in Figure 38. As shown in this figure, the top layer of baked bread at 9 minutes has the highest amount of QDs-anti-gliadin and therefore the highest amount of gliadin. The center layer of baked bread at 5 minutes shows the lowest amount of gliadin. As shown in Figure 38, the top layer of both baked bread contains more gliadin than the uncooked dough sample. The uncooked dough sample also, has more gliadin than bottom

layers of baked bread at 9 and 5 minutes. These results indicate that heat plays an important role on distribution of gliadin in baked bread samples.

Sample CSLM images of the cooked flat bread samples and the dough are shown in Figure 39. We can see that the fluorescence intensities observed in these figures follow the average values in Figure 38 reasonably consistently but not perfectly.

Also, as shown in the top layer of baked bread at 9 minutes in Figure 39, gliadin proteins present in both bulk and the gas cell wall which is consistent with the results obtained by Li et al. (2007). Also the results show the differences in distribution of gliadin proteins in different samples and different layer of samples. Differences in distribution of gold labeled antibody were observed by Lindsay and Skerritt (2000) in gliadin, low molecular weight glutenin subunits (LMW-GS) and high molecular weight subunits (HMW-GS) indicated that there are differences in the distribution of the different glutenin subunits and gliadin in wheat flour dough. Their result expressed the possible mechanisms of HMW-GS, LMW-GS and gliadins affect dough properties. Also, Gan et al. (1990) and Parker et al. (1990) concluded that during dough formation, the stretched gluten proteins become aligned burying the epitopes in the gluten and making them inaccessible to antibody.

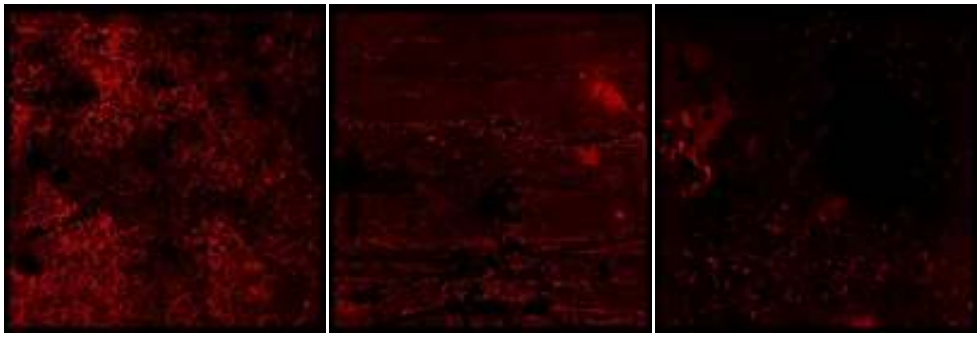

a b c

Figure 36. Sample 3-D fluorescence intensity profile of QDs-gliadin antibody conjugated images of a 400 μm x400 μm area a) top layer, b) center layer and c) bottom layer of baked bread at 9 minutes.

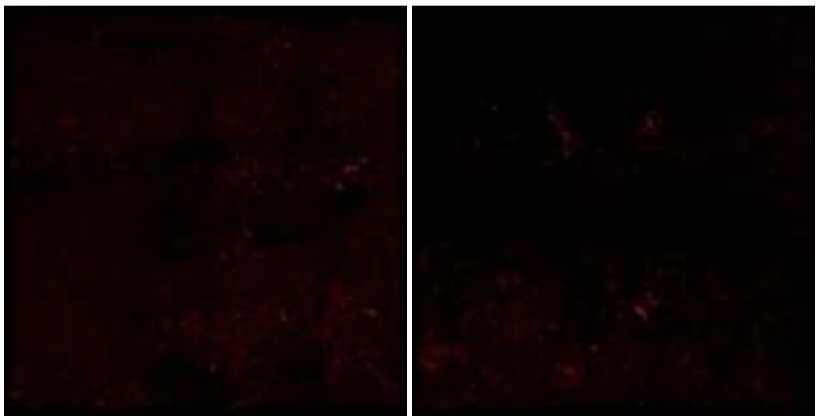

a b

Figure 37. Sample 3-D fluorescence intensity profile of QDs-gliadin antibody conjugated images of dough sample for selected image 400 μmx 400 μm in size in a) section 3 and b) section 4 of sample.

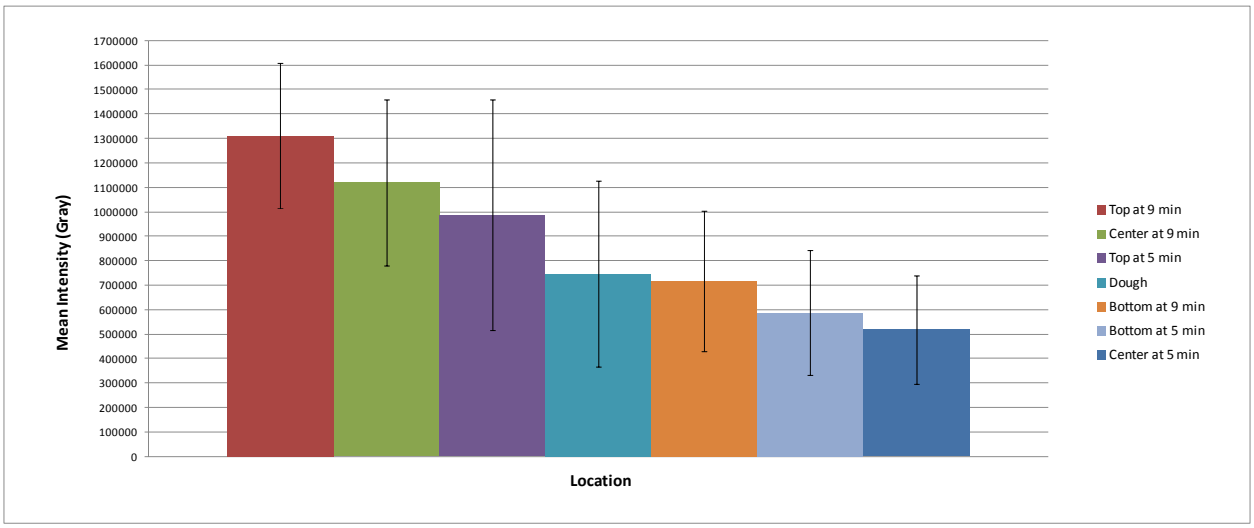

Figure 38. Mean intensity values of gliadin in 7 samples.

Table 2. Sum intensity values of QDs-gliadin antibody conjugate in Section 3 and Section 4 of dough sample

Sample	**Sum intensity (Gray)**
Section 3 of dough sample	769973
Section 4 of dough sample	444575

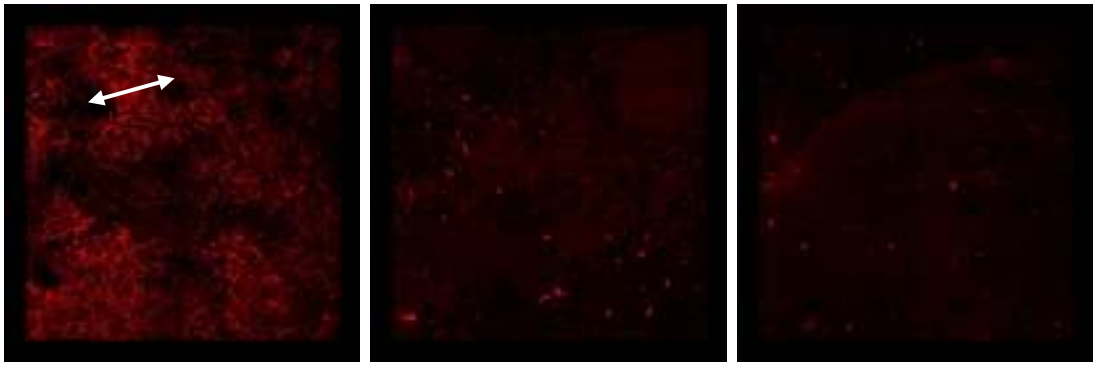

a b c

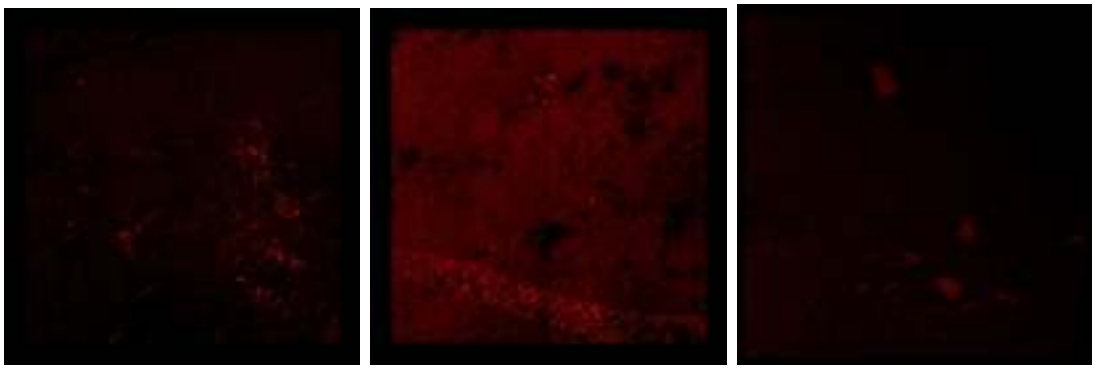

d e f

g

Figure 39. The representative 3-D fluorescence intensity profiles of QDs gliadin antibody conjugated images from the highest value to lowest value for seven samples a) top layer of baked bread at 9 min b) center layer of baked bread at 9 min c) top layer of baked bread at 5 min d) dough e) bottom layer of baked bread at 9 min f) bottom layer of baked bread at 5 min g) center layer of baked bread at 5 min. Arrow show the gas cell.

4.2. ANOVA Test Results

The ANOVA test with two significance level of α=0.05 and α=0.01 was applied to investigate whether the mean intensity values of gliadin for all samples are the same or not. Also, in order to understand whether the mean intensity values of gliadin in 4 different sections differ in each 7 samples, the ANOVA test with single factor was performed. The result of ANOVA test at α =0.05 and α=0.01 is presented in Table 3. Moreover, the ANOVA test for two by two different section in each sample was performed to understand whether the interaction between two different sections have an effect on distribution of gliadin proteins. The result is shown in Table 4. In addition, in order to evaluate which section in the dough and baked product samples show differences in the distribution of gliadin, the ANOVA test at both significance level (α =0.05 and α=0.01) for each section in three different layers (top, center and bottom) of baked bread at 9 and 5 minutes was conducted. Table 5 shows the ANOVA result with α =0.05 and α=0.01 the difference in the distribution of gliadin in dough and baked bread at 9 and 5 minutes. The four different sections which are selected in each sample for doing the experiment and the ANOVA test results are shown in Figure 40.

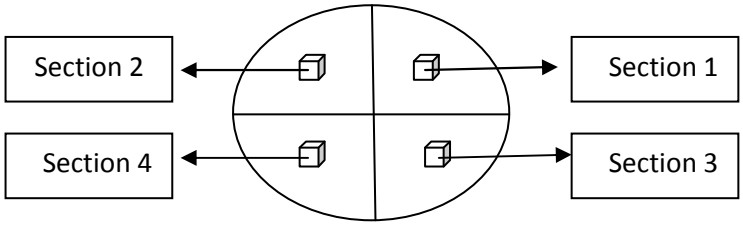

Figure 40. The four different selected sections in each sample.

Table 3. ANOVA result for distribution of gliadin in seven different samples

Sample	P-value	Result with α =0.05	Result with α =0.01
Dough	0.154217	No differences	No differences
Top layer of Baked bread at 9 min	0.24907	No differences	No differences
Center layer of Baked bread at 9 min	1.9E-08	Significant differences	Significant differences
Bottom layer of Baked bread at 9 min	0.000488	Significant differences	Significant differences
Top layer of Baked bread at 5 min	5.9E-05	Significant differences	Significant differences
Center layer of Baked bread at 5 min	0.000185	Significant differences	Significant differences
Bottom layer of Baked bread at 5 min	0.000253	Significant differences	Significant differences

* The highlighted regions shows significant differences for four different sections in the sample

Table 4. ANOVA result for distribution of gliadin between two by two sections in each sample with α =0.05 and α=0.01

Region/Sample	P-value	Result with α =0.05	Result with α =0.01
1 & 2/Top baked bread at 9 min	0.954987	No differences	No differences
1 & 3/Top baked bread at 9 min	0.229662	No differences	No differences
1 & 4/Top baked bread at 9 min	0.356958	No differences	No differences
2 & 3/Top baked bread at 9 min	0.307506	No differences	No differences
2 & 4/Top baked bread at 9 min	0.368765	No differences	No differences
3 & 4/Top baked bread at 9 min	0.010503	Significant differences	No differences
1 & 2/Center baked bread at 9 min	0.023074	Significant differences	No differences
1 & 3/Center baked bread at 9 min	0.016351	Significant differences	No differences
1 & 4/Center baked bread at 9 min	0.000235	Significant differences	Significant differences
2 & 3/Center baked bread at 9 min	5.88E-06	Significant differences	Significant differences
2 & 4/Center baked bread at 9 min	0.016727	Significant differences	No differences
3 & 4/Center baked bread at 9 min	8.27E-08	Significant differences	Significant differences
1 & 2/Bottom baked bread at 9 min	0.036054	Significant differences	No differences
1 & 3/Bottom baked bread at 9 min	0.003929	Significant differences	Significant differences
1 & 4/Bottom baked bread at 9 min	0.000122	Significant differences	Significant differences
2 & 3/Bottom baked bread at 9 min	0.277866	No differences	No differences

Table 4 (cont.)

Region/Sample	P-value	Result with α =0.05	Result with α =0.01
2 & 4/Center baked bread at 5 min	0.175385	No differences	No differences
3 & 4/Center baked bread at 5 min	0.293925	No differences	No differences
1 & 2/Bottom baked bread at 5 min	5E-08	Significant differences	Significant differences
1 & 3/ Bottom baked bread at 5 min	0.59601	No differences	No differences
1 & 4/ Bottom baked bread at 5 min	0.000167	Significant differences	Significant differences
2 & 3/ Bottom baked bread at 5 min	0.008883	Significant differences	Significant differences
2 & 4/ Bottom baked bread at 5 min	0.088	No differences	No differences
3 & 4/ Bottom baked bread at 5 min	0.085233	No differences	No differences
1 & 2/Dough	0.623517	No differences	No differences
1 & 3/Dough	0.677949	No differences	No differences
1 & 4/Dough	0.110172	No differences	No differences
2 & 3/Dough	0.838429	No differences	No differences
2 & 4/Dough	0.000191	Significant differences	Significant differences
3 & 4/Dough	0.000805	Significant differences	Significant differences

* The highlighted regions have different result in α =0.05 and α=0.01

Table 5. ANOVA result for distribution of gliadin in four sections in different layers of baked breads at 9 minutes and 5 minutes

Region/Sample	P-value	Result with α =0.05	Result with α =0.01
Section 1/ Top, Center and Bottom of baked bread at 9 min	0.083442	No differences	No differences
Section 2/ Top, Center and Bottom of baked bread at 9 min	0.000925	Significant differences	Significant differences
Section 3/ Top, Center and Bottom of baked bread at 9 min	7.52E-10	Significant differences	Significant differences
Section 4/ Top, Center and Bottom of baked bread at 9 min	5.36E-07	Significant differences	Significant differences
Section 1/ Top, Center and Bottom of baked bread at 5 min	7.98E-09	Significant differences	Significant differences
Section 2/ Top, Center and Bottom of baked bread at 5 min	1.11E-06	Significant differences	Significant differences
Section 3/ Top, Center and Bottom of baked bread at 5 min	0.100093	No differences	No differences
Section 4/ Top, Center and Bottom of baked bread at 5 min	0.092054	No differences	No differences

* The highlighted regions shows significant differences in each section of baked bread samples.

As shown in Table 3, the mean intensity values of gliadin in four different selected sections in all samples except dough and top layer of baked bread at 9 minutes have statistically significant differences. For example, in center layer of baked bread at 9 minutes, the average intensity of gliadin in section 3 is 1497084 Gray, which is higher than section 4 with average intensity of gliadin of 749259.1 Gray. The average intensity values of gliadin are shown in Table 6.

Table 6. The average intensity values of QDs-gliadin antibody conjugate in all samples.

Sample	**Average intensity of QDs-gliadin antibody conjugate (Gray)**
Top layer of baked bread at 9 min	
Section 1	1300656
Section 2	1310208
Section 3	1458512
Section 4	1175073
Center layer of baked bread at 9 min	
Section 1	1243195
Section 2	987535.3
Section 3	1497084
Section 4	749259.1
Bottom layer of baked bread at 9 min	
Section 1	1008381
Section 2	734866.7
Section 3	601640.3
Section 4	522251.6
Top layer of baked bread at 5 min	
Section 1	1499505
Section 2	1013777
Section 3	814180.8
Section 4	617309.3
Center layer of baked bread at 5 min	

Table 6 (cont.)

Sample	Average intensity of QDs-gliadin antibody conjugate (Gray)
Section 1	761960.4
Section 2	494565.9
Section3	451384.7
Section 4	366802.8
Bottom Layer of baked bread at 5 min	
Section 1	779116
Section 2	365452.9
Section 3	717427.6
Section4	487767.2
Dough	897954.7
Section 1	
Section 2	780764.7
Section 3	797371.4
Section 4	507285.7

Based on Table 3, there is no statistically significant difference in mean intensity of gliadin in 4 different sections of top layer of baked bread at 9 minutes. The data in Table 4, also shows no significant difference between mean intensity values of gliadin in section 1 & 2, section 1 & 3, section 1 & 4, section 2 & 3, section 2 & and 4 and section 3 & 4. Although there are no significant differences in mean intensity values of gliadin in 4 different sections in dough sample based on the result in Table 3, the statistically significant difference was observed in mean intensity values of gliadin between section 2 & 4 and section 3 & 4 based on the data in Table 4. The mean intensity value of gliadin in section 2 is 780764.7 Gray, which is higher than the mean intensity value of gliadin in section 4 (507285.7 Gray) and lower than section 3 (797371.4 Gray) in dough sample. Therefore, the interaction between section 2 & 4 and section 3 & 4 have an influence on the intensity of QDs-gliadin antibody conjugate in dough sample.

However, the different sections and even the interaction between the sections have no effect on the distribution of gliadin in top layer of baked bread sample at 9 minutes. It can be concluded that heat plays an important role in distribution of gliadin proteins in samples. Also, the result shows no significant difference in mean intensity values of gliadin between section 3 & 4 in bottom layer of both baked bread at 9 and 5 minutes which it means the interaction of these two sections has no effect on distribution of gliadin. However, in dough sample the interaction section 3 & 4 is important in gliadin distribution.

The data in Table 5 indicates in which section the mean intensity values of gliadin in three layers of baked bread at 9 minutes and three layer of baked bread at 5 minutes show considerable differences. With regard to three layers of baked bread at 9 minutes, in all sections except section 1, the mean intensity values of gliadin at both significance levels are different. In both sections 2 and 4, the mean intensity value of gliadin in top layer higher than center and center layer is higher than bottom layer in baked bread at 9 minutes. However, in section 3, the mean intensity of gliadin in center layers is more than top layer and top is more than bottom layer in baked bread at 9 minutes. The average intensity values of QDs-gliadin antibody conjugate is shown in Table 6. In three layers of baked bread at 5minutes among four selected sections only section 1 and section 2 represents significant differences in mean intensity values of gliadin. In both sections (2 and 3) the mean intensity value of gliadin in top layer is higher than the center layer and the center layer is higher than bottom layer in baked bread at 5 minutes. Therefore, in section 2 and 4 of baked bread at 9 minutes and also in section 2 and 3 of baked bread at 5 minutes heat has an effect on distribution of gliadin. So that top layer with farthest distance to heat in compare to center and bottom layer contains more gliadin than them.

In addition, the ANOVA test to indicate whether the mean intensity values of gliadin with respect to different samples, dough and baked bread at 9 minutes and also dough and baked bared at 5 minutes at two significance levels α =0.05 and α=0.01 was performed. The result is shown in Table 7. The data in this table with probability 95% (α =0.05) show the difference in mean intensity value of gliadin in comparison of dough and baked bread at 9 minutes and also between dough and baked bread at 5 minutes. Also, with probability 99% (α =0.01) the mean intensity value of gliadin in dough and baked bread at 9 minutes are significantly difference. Therefore, the distribution of gliadin protein can be influenced by different samples. However, at significance level α =0.0, there is no significant difference in distribution of gliadin between dough and baked bread at 5 minutes. Based on all data, it can be concluded that different sections, interaction between two section, heat and different samples play an important role in distribution of gliadin proteins in dough and baked bread samples.

Table 7. ANOVA result for comparison of distribution of gliadin in dough and two different baked breads

Sample	**P-value**	**Result with α =0.05**	**Result with α =0.01**
Dough and Baked bread at 9 min	5.9358E-05	Significant differences	Significant differences
Dough and Baked bread at 5 min	0.039391	Significant differences	No differences

4.3. Discussion

The gluten proteins, and their subfractions, gliadin and glutenin are very important for wheat flour and baked bread functionality. They undergo changes during heat treatment involving sulfhydryl group (SH) which are converted to S-S bonds. In addition air cells grow to give the foam like structure and the strength of the gluten network and its subfractions glutenin and gliadin play a major role in the development of this structure. The changes in proteins are

also coupled with gelatinization of starch which affects the distribution of the protein network and its integrity in the bread matrix. Usually glutenin gives the stiffer network because of the high density of intra and inter molecular disulfide bonds but gliadin has the ability to stretch and flow because there are fewer intramolecular disulfide bonds. The complex interaction between all these changes affects the quality of the final baked product. Gliadin is a smaller molecule without free SH moieties. However, glutenin is a large molecule containing many inters and intramolecular S-S bonds in addition to free SH groups (Rumbo et al., 2001). Gliadin is a heterogeneous mixture of proteins containg α, β, γ and ω-gliadins. All cysteine residues in gliadin fractions except ω-gliadins are involved in intrachain disulfide (S-S) bonds. In contrast, ω-gliadins lack cysteine residues. Disulfide linkages in gliadin are primarily intramolecular, whereas in glutenin they are both intermolecular and intramolecular.

The changes induced by heat eventually lead to large gluten protein aggregates with formation gliadin-glutenin bonds through S-S cross links. The SH-SS exchange mechanism requires free SH groups. Therefore, changes in the level of SH during hydrothermal treatment should affect gliadin-glutenin association. These groups increase the level of gliadin-glutenin cross linking at higher temperature (Lagrain et al., 2008). Also, Hayta et al. (2005) showed the glaidin proteins were not affected at lower temperature but at temperature greater than 70°C these proteins also undergo chemical changes, apparently, involving SH group reactions. Madeka and Kokini (1994) demonstrated a networking reaction for gliadin with 15-40% moisture in the temperature range of 70-115°C. Gliadin behaved likes an entangled fluid below this temperature. Also, they showed the maximum crosslinking density for gliadin at 100°C using G' and density data. The aggregated gliadin was softened when the temperature exceeded 135°C.

Based on all results, differences in the distribution of QDs-gliadin antibody indicate that there are differences in the distribution of gliadin protein between dough and baked bread samples. The heating time is also an important factor in the distribution of gliadin. Because two different heating times showed significant difference in the distribution of gliadin between baked bread at 9 minutes and baked bread at 5 minutes. Previous studies showed the heat treatment increases the disulfide-sulfhydryl exchange, promoting the formation of intermolecular bridges in sulfur-rich gliadin and the extractability of gliadin decreases (Rumbo et al., 2001 and Lagrain et al., 2008). The lower intensity values of gliadin in bottom layers which are closest to direct heat in baked bread samples confirm these results. The possible explanation for this result is the fact that the character of gliadin changes under high heat and becomes a network which is not recognizable by the antibody anymore giving lower fluorescence intensity values.

In this study, the subfarctions of gliadin cannot be distinguished by the antibody when gliadin excessively netwroks between itself or crosslinks with glutenin. However, ω-gliadins do not contain SH group, therefore they are not involved in SH-SS exchange reaction. Rumboo et al. (2001) showed the relative area of ω-gliadins increases from 14% in unheated dough or flour to 28% in the extracts from dough heated at 160°C for 20 minutes.

It is worth mentioning that the heat has drastic effect on protein structure and may produce changes in the epitopes which are recognized by antibody. Therefore, the detection can be affected. Moreover, the unavailability of the epitopes to the antibodies results in the poor binding capacity of the antibodies. Gliadin are monomers, they may fill the space around the large glutenin polymer, which reduce the availability of the epitope on the protein (Lindsay and Skerritt., 2000). Ponomarev and Lifanova (1956) found that the denaturation depends not only on temperature, but also on duration of heating. They showed the rate constant of heat denaturation

of gliadin changes very little with time of denaturation, but increases with temperature of denaturation.

Although no fixation technique was used in this project, it can not guarantee that the structures of samples do not change. Lindsay and Skerritt (2000) expressed the N-terminal domain contains a high portion of disulfide bound, they would be highly folded. Several of the gliadin selective antibodies typically recognized epitopes in the N-terminal domain, which is highly folded and therefore less accessible.

Chapter Five:

Conclusion

Quantum dots conjugated with various biological markers such as antibodies that recognize proteins has been used in variety of bioanalytical and biomedical applications. This technology has been used in this paper to understand the behaviour of gliadin in a cereal matrix for the first time. We used this novel perspective of QDs application as a fluorescence probe to track the distribution of gliadin proteins in dough and flat bread and the effect of heat on its distribution. We showed the distribution of gliadin protein changes between the dough and bread samples with two different baking times. Also, the distribution of gliadin protein changes between the four different sections in each sample and between the three different layers in baked bread samples. In addition, the interaction between two sections and heat play an important role in distribution of gliadin proteins in dough and baked bread samples.

References:

Akerman, M. E., Chan, W.C., Laakkonen, P., Bhatia, S. N., Ruoslahti, E. 2002. Nanocrystal targeting in vivo. Proc. Nat. Acad. Sci. USA. 99, 12617.

Altenbach,S, B., Kothari, K, M. 2007. Omega gliadin genes expressed in Triticum aestivum cv. Butte 86: effects of post-anthesis fertilizer on transcript accumulation during grain development. J Cereal Sci, 46,169.

Ang, S., Kogulanathan, J., Morris, G. A., Ko¨k, M.S., Shewry, P.R., Tatham, A. S., Adams, G, G., Rowe, A, J., Harding, S. A. 2010. Structure and heterogeneity of gliadin: a hydrodynamic Evaluation. Eur Biophys J, 39, 255.

Autran, J. C., Bourdet, A. 1975. L'identification des varieties de ble: etablissmaent d'un tableau general de determination fonde sur le diagramme electrophoretique de gliadins du grain. Ann. Amelior. Plantes, 25, 277 (in French).

Autran, J. C., Bushuk, W., Wrigley, C. W., Zillman, R. R. 1979. Wheat cultivar identification by gliadin electrophoregrams. IV. Comparison of international methods. Cereal Foods World, 24, 471.

Ballou, B., Lagerholm, B. C., Ernst, L. A., Bruchez, M. P., Waggoner, A. S. Noninvasive imaging of quantum dots in mice. Bioconjug. Chem. 15, 79.

Bentzen, E.L., House, F., Utley, T. J., Crowe, J. E., Wright, D. W. 2005. Progression of Respiratory Syncytial Virus Infection Monitored by Fluorescent Quantum Dot Probes. Nano Letters, 5, 591.

Bietz, J. A., Burnouf, T. 1985. Chromosomal control of wheat gliadin: Analysis by reversed-phase high-performance liquid chromatography. Theor. Appl. Genet. 20, 599.

Bugusu, B. A., Rajwa, B., Hamaker, B. 2001. Interaction of maize zein with wheat gluten in composite dough and bread as determined by confocal laser scanning microscopy. Scanning, 24, 1-5.

Cao, Y. A., Yang, K., Li, Z.G., Zhao, C., Shi, C. M., Yang, J. 2010. Near-infrared quantum-dot-based non-invasive in vivo imaging of squamous cell carcinomaU14. Nanotechnology, 21.

Chan, P. M., Yuen, T., Ruf, F., Gonzalez-Maeso, J., Sealfon, S. C. 2005. Method for multiplex cellular detection of mRNA usng quantum dot fluorescent in siyu hybridization. Nucleic Acids Res, 33.

Chen, Z., Li, G., Zhang, L., Jiang, J., Li, Z., Peng, Z., Deng, L. 2008. A new method for the detection of ATP using a quantum-dot-tagged aptamer. Anal. Bioanal. Chem. 392, 1185.

Cole, E, W., Kasarda, D, D., Lafiandra, D. 1984. The conformational structure of a-gliadin. Intrinsic viscosities under conditions approaching the native state and under denaturing conditions. Biochim Biophys Acta, 787, 244.

Cui, B., Wu, C., Chen, L., Ramirez, A., Bearer, E. L., Li, W. P., Mobley, W. C., Chu, S. 2007. One at a time, live tracking of NGF axonal transport using quantum dots. Proc. Natl. Acad. Sci. USA. 104, 13666.

Dahan, M., Levi, S., Luccardini, C., Rostaing, P., Riveau, B., Triller, A. 2003. Diffusion dynamics of glycine receptors revealed by single-quantum dot tracking. Science, 302, 442.

Drbohlavova, J., adam, V., Kizek, R., Hubalek, J. 2009. Quantum dots- Characterization, preparation and usage in biological system. Int. J. Mol. Sci. 10, 656.

DuCros, D. L., Wrigley, C. W. 1979. Improved electrophoretic methods for identifying cereal varieties. J. Sci. Food Agric. 30, 785.

Durrenberger, M. B., Handschin, S., Conde-Petit, B., Escher, F. 2001. Visulization of food structure by confocal laser scanning microscopy (CLSM). Lebensm-Wiss. u- Technol, 34, 11-17.

Entrikin, P, P.1941. Dielectric behaviour of solutions of the protein gliadin. J Am Chem Soc, 63, 2127.

Erogbogbo, F., Yong, K. T., Roy, I., Xu, G. X., Prasad, P. N., Swihart, M. T. 2008. Biocompatible luminescent silicon quantum dots for imaging of cancer cells. ACS Nano, 3, 502.

Field, J, M., Tatham, A, S., Baker, A., Shewry, P, R. 1986. The structure of C hordein. FEBS Lett, 200, 76.

Freeman, T. P., Shelton, D. R., Bjerke, J. M., Skierkowski, K. 1991. The ultrastructure of wheat gluten: variation related to sample preparation. Cereal Chem. 68 (5), 492-498.

Gan, Z., Angold, R. E., Williams, M. R., Ellis, P. R. Vaughan, J. G. Galliard, t. 1990. The microstructure and gas retention of bread dough. J Cereal Sci. 12, 15-24.

Gao, X., Cui, Y., Levenson, R. M., Chung, L.W. K., Nie, S. 2004. In vivo cancer targeting and imaging with semiconductor quantum dots. Nat. Biotech. 22, 969.

Gerion, D., Parak, W. J., Williams, S. C. Zanchet, D., Micheel, C. M., Alivisatos, A. P. 2002. Sorting fluorescent nanocrystal with DNA. J. Am. Chem. Soc. 124, 7070.

Goldman, E. R., Anderson, G. P., Tran, P. T., Mattoussi, H., Charles, P. T. Mauro, J. M. 2002. Conjugation of luminescent quantum dots with antibodies using an engineered adaptor protein to provide new reagents for fluoroimmunoassays. Anal. Chem. 74, 841.

Goldman, E. R., Clapp, A. R., Anderson, G. P., Uyeda, H. T., Mauro, J. M., Medintz, I. L., Mattoussi, H. 2004. Multiplexed toxin analysis using four colors of quantum dots fluororeagents. Ana. Chem. 76, 684.

Guerrieri, N., alberti, E., Lavelli, V., Cerletti, P. 1996. Use of spectroscopic and fluorescence techniques to assess heat induced modifications of gluten. Cereal Xhem, 73, 368-374.

Halpert, J, E., Porter, V, J., Zimmer, J, P., Bawendi, M, G. 2006. Synthesis of CdSe/CdTe Nanobarbells. J Am Chem Soc. 128, 12590.

Han, M, Y., Gao, X., Su, J, Z., Nie, S, M. 2001. Quantum-dot-tagged microbeads for multiplexed optical coding of biomolecules. Nat Biotechnol, 19,631.

Hayta, M., Schofield, J. D. 2005. Dynamic rheological behavior of wheat glutens during heating. J Sci Food, 85, 1992-1998.

Hankaki, K., Momo, A., Oku, T., Komoto, A., Maenosono, S., Yamaguchi, Y, et al. 2003. Semiconductor quantum dot/albumin complex is a long-life and highly photostable endosome marker. Biochem. Biophys. Res. Commun, 302, 496.

Hoshino, a., Fujioka, K., Oku, T., Nakamura, S., Suga, M., Yamaguchi, Y et al. 2004. Quantum dots targeted to the assigned organelle in living cells. Microbiol Immunol, 48, 985.

Hoseney, R. C., Finney, K. F., Pomeranz, Y. 1970. Functional (breadmaking) and biochemical properties of wheat flour components. VI. Gliadin-lipid-glutenin interaction in wheat gluten. Cereal Chem, 47, 135-140.

Hsia , C, C., Anderson, O, D. 2001. Isolation and characterization of wheat x-gliadin genes. Theor Appl Genet, 103, 37.

Hua, X. F., Liu, T. C., Cao, Y. C., Liu, B., Wang, H. Q., Wang, J. H., Huang, Z. L., Zhao, Y. D. 2006. Characterization of the coupling of quantum dots and immunoglobulin antibodies. Anal Bioanal Chem, 386, 1665-1671.

Jaiswal, J. K., Mattoussi, H., Mauro, J. M., Simon, S. M. 2003. Long-term multiple color imaging of live cells using quantum dot bioconjugates. Nat. Biotechnol. 21, 47.

Jamieson, T., Bakhshi, R., Petrova, D., Pocock, R., Imani, M., Seifalian, A. M. 2007. Biological applications of quantum dots. Biomaterials, 28, 4717.

Jankiewicz, M., Pomeranz, Y. 1965. Comparison of the effect of N-ethylmaleimide and urea on rheological properties of dough, Cereal Chem, 42, 37.

Jin, S., Hu, Y., Gu, Z., Liu, L., Wu, H. C. 2011. Application of quantum dots in biological imaging. J Nanomaterials, 2011, 1-13.

Kasarda, D. D., Bernardin, J. E., Qualset, C. O. 1976. Relationship of gliadin protein components to chromosomes in hexaploid wheats (*Triticum aestivum* L.) Proc. Natl. Acad. Sci. U. S. A. 73, 3646.

Kloepfer, J. A., Mielke, R. E., Wong, M. S., Nealson, K. H., Stucky, G., Nadeau, J. L. 2003. Quantum dots as strain- and metabolism-specific microbiological labels. Appl. Environ. Microbio. 69, 4205.

Klostranec, J. M., Chan, W.C.W. 2006. Quantum dots in biological and biomedical research: recent progress and present challenges. Advanced Materials, 18,1953.

Kokini, J. L., Cocero. A. M., Madeka, H., de Graaf, E. 1994. The development of state diagrams for cereal proteins. Trends in Food Science and Technology, 5, 281- 288.

Krejci, I., Svedberg, T. 1935. The ultracentrifugal study of gliadin. J Am Chem Soc, 57, 946.

Lagrain, B., Thewissen, B. G., Brijs. K., Delcour, J. A. 2008. Mechanism of gliadin-glutenin cross-linking during hydrothermal treatment. Food Chem, 107, 753-760.

Lamm, O., Poulsen, A. 1936. The determination of diffusion constants of protein by a refractometric method. Biochem J, 30, 528.

Larre, C., Popineau, Y., Loisel, W. 1991. Fractionation of gliadins from common wheat by cation exchange FPLC. J. Cereal Sci. 14, 231.

Larson, D. R., Zipfel, W. R., Williams, R. M., Clark, S. W., Bruchez, M. P., Wise, F. W., Webb, W. W. 2003. Water-soluble quantum dots for multiphoton fluorescence imaging in vivo, Science, 300, 1434.

Lasztity, R. 1996. The Chemistry of Cereal Proteins, 2nd ed, CRC, Press: bOca Raton.

Lasztity, R. 1972. Recent results in cereal protein research, Period. Polytech. (Tech. Univ. Budapest) 16, 331.

Leszczynska, J., Lacka, a., Bryszewska, M., Brzezinska-Blaszczyk, E. 2008. The usefulness rabbit anti-QQQPP peptide antibodies to wheat flour antigenicity studies. Czech J. Food Sci, 26,24-30.

Li, W., Dobraszczyk, B. J., Wilde, P. J. 2004. Surface properties and locations of gluten proteins and lipids revealed using confocal scanning laser microscopy in bread dough. J Cereal Sci, 39, 403-411.

Li, H., Shih, W.Y., Shih, W. H. 2007. Synthesis and characterization of aqueous carboxyl-capped CdS quantum dots for bioapplications. Industrial and Engineering Chemistry Research, 46, 2013.

Li, Q. Y., Ji, K. M., Song, X. Y., Zhang, E. Y., Pei, Y. H., Yan,Y. M. 2008. Polyclonal antibodies to grain gliadins and their application in wheat quality prediction. Cereal Reaseach Communications, 36 (1), 117-124.

Lindsay, M., Skerritt, J. H. 2000. Immunocytochemical localization of gluten proteins uncovers structural organization of glutenin macropolymer. Cereal Chem, 77 (3), 360-369.

Lookhart, G. L., Jones, B. L., Hall, S. B., Finney, K. F. 1982. An improved method for standardizing polyacrylamide gel electrophorsis of wheat gliadin proteins. Cereal Chem, 59, 178.

Loussert,C., Popineau, Y., Mangavel,C. 2008. Protein bodies ontogeny and localization of prolamin components in the developing endosperm of wheat caryopses. Journal of Cereal Science, 47, 445-456.

Macritchie, F. 1992. Physiochemical properties of wheat proteins in relation to functionality. Advances in Food and Nutrition Research. J. E. Kinsella, eds. Academic Press: London, 1-87.

Madeka, H., Kokini, J. L. 1994. Changes in rheological properties of gliadin as a function of temperature and moisture: development of a state diagram. J. Food Eng, 22, 241.
Magnus, E. m., Brathen, E., Sahlstrom, S., Vogt, G., Faergestad, E. M. 2000. Effects of flour composition, physical dough properties and baking process on hearth loaf properties studied by multivariate statistical methods. J. Cereal Sci, 32, 199-212.

Matsuo, H., Kohno, K., Morita, E. 2005. Molecular cloning, recombinant expression and IgE binding of omega-5 gliadin, a major allergen in wheat-dependent exercise-induced anaphylaxis. FEBS J, 272, 4431.

Mecham, D. K., Kasarda, D. d., Qualset, C. O. 1978. Genetic aspect of wheat gliadin proteins. Biochem. Genet. 16, 831.

Medintz, I. L., Uyeda, H. T., Goldman, E. R., Mattoussi, H. 2005. Quantum dot bioconjugates for imaging, labeling and sensing. Nature Materials, 4, 435.

Metakovsky, E. V., Graybosch, R. A. 2006. Gliadin alleles in wheat: identification and applications, Gliadin and Glutenin The Unique Balance of Wheat Quality; Wrigley, C., Bekes, F., Bushuk, W. Eds., AACC International, Minnesota, U.S.A.

Micard, V., Guilbert, S. 2000. Thermal behavior of native and hydrophobized wheat gluten, gliadin and glutenin-rich fractions by modulated DSC. Int. J. Biol. Macromol, 27, 229-236.

Miles, M. J., Carr, H. J., McMaster, T. C., I'Anson, K. J., Belton, P. S., Morris, V. J., Field, J. M., Shewry, P. R., Tatham, A. S. 1991. Scanning tunnelling microscopy of a wheat seed storage protein reveals details of an unusual supersecondary structure. Proc. Natl. Acad. Sci. (Biochem.) 88, 68.

Novoselskaya, A. Y., Metakovsky, E. V., Sozinov, A. A. 1983. The study of gliadin polymorphism of some wheat varieties by means of one- and two-dimensional electrophoresis. Tsitologia Genet. 17, 45 (in Russian).

Orth, R. A., Bushuk, W. 1972. A comparative studies of the proteins of wheats of diverses baking quality. Cereal Chem. 49, 268.

Parker, M. L., Mills, E. N. C., Morgan, R. A. 1990. The potential of immunoprobes for loacating storage proteins in wheat endosperm and bread. J Science and Food Agriculture, 52, 35-45.

Pathak, S., Chio, S. K., Arnheim, N., Thmpson, M. E., 2001. Hydroxylated quantum dots as luminescent probes for in situ hybridization. J. Am. Chem. Soc. 123, 4103.

Patolsky, F., Gill, R., Weizmann, Y., Mokari, T., Banin, U., Willner, I. 2003. Lighting-up the dynamics of telomerization and DNA replication by CdSe-ZnS quantum dots. J. Am. Chem. Soc. 125, 13918.

Payne, P. I., Holt, L. M., Lawrence, G. J., Law, C. N. 1982. The genetics of gliadin and glutenin, the major storage proteins of the wheat endosperm. Qual. Plant Food Human Nutr. 31, 229.

Payne, P. I., Holt, L. M., Jarvis, M. G., Jackson, E. A. 1985. Two-dimensional fractionation of the endosperm proteins of bread wheat (*Triticum aestivum*): Biochemical and genetic studies. Cereal Chem. 62, 319.

Pezolet, M., Bononfant, S., Dousseau, F., Popineau, Y. 1992. Conformation of wheat gluten proteins: Comparison between functional and solution states as determined by infrared spectroscopy. FEBS, 299, 247.

Pinaud, F., King, D., Moore, H, P., Weiss, S. 2004. Bioactivation and Cell Targeting of Semiconductor CdSe/ZnS Nanocrystals with Phytochelatin-Related Peptides. J. Am. Chem. Soc. 126, 6115.

Pomeranz, Y. 1968. Relation between chemical composition and bread-making potentialities of wheat flour, in Advances in Food Research, Vol 16, Chichester, C. O., Mark, E. M., and Stewart, G. F., Eds., Academic Press, New York, 335.

Ponomarev, V.V. 1951. Effect of temperature on denaturation of gliadin. Biokhimiya, 16, 556.

Ponomarev, V. V., Lifanova, T. A. 1956. Heat denaturation og gliadin. All-Union Research Institute of the Baking Industry, Moscow, 576.

Qian, J., Yong, K.T., Roy, I. et al. 2007. Imaging pancreatic cancer using surface-functionalized quantum dots. Journal of Physical Chemistry, 11, 6969.

Rosenthal, S. J., Chang, J. C., Kovtun, O., McBride, J. R., Tomlinson, I. D. 2011. Biocompatible quantum dots for biological applications. Chemistry and Biology, 18, 10-24.

Rumbo, M., Chirdo, F. G., Fossati, C. A., Anon, M. C. 2001. Analysis of the effects of heat treatment on gliadin immunochemical quantification using a panel of anti-prolamin antibodies. J. Agric. Food Chem, 49, 5719-5726.

Scanlon, M. G., Bushuk, W. 1990. Application of photodiode-array detection in RP-HPLC of gliadins for automated wheat variety identification. J. Cereal Sci. 12, 229.

Schofield, J.D., Bottomley, R. C., Timms, M. F., Booth, M. R. 1983. The effect of heat on wheat gluten and the involvement of sulphydryl-disulfied interchange reactions. J Cereal Sci, 1, 241-253.

Shewry, P. R., Faulks, A. J., Pratt, H. M., Miflin, B. J. 1978. The varietal identification of single seeds of wheat by sodium dodecyl-sulphate polyacrylamide gel electrophoresis of gliadin. J. Sci. Food Agric. 29, 841.

Shewry, P. R., Tatham, A. S. (1990). The prolamin storage proteins of cereal seeds: structure and evolution. Biochem. J. 267, l- 12.

Shewry, P, R,. D'Ovidio R., Lafiandra D., Jenkins J, A., Mills ENC, Be´ke´s, F. 2008. Wheat grain proteins. In: Shewry PR, Khan K (eds) Wheat chemistry and technology, 4th edn. American Association of Cereal Chemists, St. Paul, pp 223- 298.

Scott, D, J., Schuck, P. 2005. A brief introduction to the analytical ultracentrifuge of proteins for beginners. In: Scott DJ, Harding SE, Rowe AJ (eds) Analytical ultracentrifugation. Techniques and methods. Royal Society of Chemistry, Cambridge, pp 1–25

Song, X. Y., Cai, Q. F., Gao, W. S., Liu,G. T., Huang, T. C. 1998. Immunochemical assay for quality and immunological homology of storage proteins in different closely related genera and species of wheat. Acta Bot. sin, 40, 527.

Sozer, N., Sivaguru, M., Kokini, J. L. 2012. Use of quantum nanodot crystals as imaging probes for cereal proteins. Submitted to J Food Engineering.

Stathopoulos, C. E., Tsiami, A. A., Dobraszczyk, B. J., Schofield, J. D. 2006. Effect of heat on rheology of gluten fractions from flours with different bread-making quality. J Cereal Sci, 43, 322.

Stathopoulos, C. E., Tsiami, A. A., Schofield, J. D., Dobraszczyk, B. J. 2008. Effect of heat on rheology, surface hydrophobicity and molecular weight distribution of glutens extracted from flours with different bread-making quality. J Cereal Sci, 47, 134-143.

Tada, H., higuchi, H., wanatabe, T. M., Ohuchi, N. 2007. In vivo real-time tracking of single quantum dots conjugated with monoclonal anti-HER2 antibody in tumors of mice. Cancer Res. 67, 1138.

Tatham, A., Shewry, P. R. 1985. The conformation of wheat gluten proteins. The secondary structure and thermal stabilities of α -, β -, γ -,and ω -gliadins. J. Cereal Sci. 3, 103.

Tatham, A, S., Shewry, P, R. 1995. The S-poor prolamins. J Cereal Sci, 2, 99.

Taylor, N, W., Cluskey, J, E. 1962. Wheat gluten and its glutenin component: viscosity, diffusion and sedimentation studies. Arch Biochem Biophys, 97, 399.

Transmo, K. M., Magnus, E. M., Baardseth, P., Schofield, D., Aamodt, A., Faergestad, E. M. 2003. Comparison of small and large deformation rheological properties of wheat dough and gluten. Cereal Chem, 80 (5), 587-595.

Thomson, N, H., Miles, M, J., Popineau, Y., Harries, J., Shewry, P, J., Tatham, A, S. 1999. Small angle X-ray scattering of wheat seed storage proteins: a-, c- and x-gliadins and the high molecular weight (HMW) subunits of glutenin. Biochim Biophys Acta, 1430, 359.

Vakar, A., Pumpyanskii, A. J., Semenova, L.V. 1965. The influence of D_2O on the physical properties of gluten and wheat dough (in Russian), Prikl. Biochim, Mikrobiol, 1, 25.

Varriale, A., rossi, M., Staiano, M., Terpetschnig, E., Barbieri, B., Rossi, M., D Auria, S. 2007. Fluorescence correlation spectroscopy assay for gliadin in food. Anal. Chem, 79, 4687-4689.

Vashist, S. K., Tewari, r., Bajpai, R. P., Bharadwaj, L. M., Raiteri, R. 2006. Review of quantum dot technologies for cancer detection and treatment. J Nanotechnology Online. http://www.azonano.com/article.aspx?ArticleID=1726

Wall, J.S. 1971. Disulfied bonds: determination, location, and influence on molecular peoperties of proteins. J. Agr. Food Chem, 19, 620.

Wall, J.S. 1979. The role of wheat proteins in determining baking quality, in Recent Advances in the Biochemistry of Cereals, Laidman, D. L., Jones, R. G. W. Eds., Academic Press, New York, 275.

Walling, M. A., Novak, J. A., Shepard, J. R. E. 2009. Quantum dots for live cell and in vivo imaging. Int. J. Mol. Sci. 10, 441.

Warren, C, C., Dustin, J, M., Xiaohu, G., Robert, E, B., Mingyong, H., Shuming, N. 2002. Luminescent quantum dots for multiplexed biological detection and imaging. Current Opinion in Biotechnology, 13, 40.

Weegels, P. L., Verhoek, J. A., de Groot, A. M. G., Hamer, R. J. 1994a. Effects on gluten of heating at different moisture contents. I. changes in functional properties. J Cereal Sci, 19, 31-38.

Wieser. H. 2007. Chemistry of gluten proteins. Food Microbiol. 24, 115-119.

Wrigley, C. W. 1970. Protein mapping by combined gel electrofocusing and electrophoresis: Application to study of genotypic variation in wheat gliadins. Biochem. Genet. 4, 509.

Wrigley, C. W., Lawrence, G. J., Shepherd, K. W. 1982. Association of Glutenin Subunits With Gliadin Composition and Grain Quality in Wheat. Australian Journal of Plant Physiology 9,15

Wrigley, C., Bekes, F., Bushuk, W. 2006. Gliadin and glutenin the unique balance of wheat quality. AACC International, St. Paul, Minnesota.

Woychik, J. H., Boundy, J. A., Dimler, R. J. 1961. Starch gel electrophoresis of wheat gluten proteins with concentrated urea. Arch. Biochem. Biophys. 94, 477.

Wrigley, C. W. 1970. Protein mapping by combined gel electrofocusing and electrophoresis: Application to study of genotypic variation in wheat gliadins. Biochem. Genet. 4, 509.

Wu, Y,V., Dimler, R, J. 1964. Conformational studies of wheat gluten, glutenin and gliadin in urea solutions at various pH's. Arch Biochem Biophys, 107,435.

Wu, X., Liu, H., Liu, J., Haley, K. N., Treadway, J. A., Larson, J. P., Ge, N., Peale, F., Bruchez, M. P. 2002. Immunofluorescent labeling of cancer marker Her2 and other cellular targets with semiconductor quantum dots. Nat. Biotech, 21, 41.

Yong, K. T., Hu, R., Roy. I. et al. 2009. Tumor targeting and imaging in live animals with functionalized semiconductor quantum dots, ACS Applied Materials and Interfaces, 1, 710.

Xing, Y., Xia, Z., Rao, J. 2009. Semiconductor quantum dots for biosensing and in vivo imaging. IEEE Transactions on Nanobioscience, 8, 4.

Zhu, L., Ang, S., Liu, W.T. 2004. Quamtum dots as a novel immunfluorescent detection system for *Cryptosporidium parvum* and *Giardia lamblia*. App. Environ. Microbiol, 70, 597.